sich zwischen der Zahl der Kettenbrüche N_B und der Zahl der absorbierten Sauerstoffmolekeln N_{O_2} folgende Beziehung:

$$N_B : N_{O_2} \approx 0{,}6 \,. \qquad [4]$$

Die Molekulargewichtsmessungen lieferten für $N_B : N_{O_2}$ Werte zwischen 0,68 und 0,84 (Tab. 2). Wenn man berücksichtigt, daß die Häufigkeit der einzelnen Zerfallsreaktionen sicher nicht unabhängig von der Temperaturführung ist, andererseits die thermische Behandlung bei den UR-Messungen und den Molekulargewichtsmessungen aus experimentellen Gründen verschieden war, sind diese Ergebnisse als eine weitere Bestätigung der Gültigkeit der angegebenen Zerfallsreaktionen zu betrachten.

Gleichzeitig ist damit gezeigt, daß der Abbau, den bestrahltes Paraffin unter der Einwirkung von Sauerstoff erleidet, auf den Zerfall der im Verlauf der Kettenreaktion [2a], [2b] gebildeten Hydroperoxy-Gruppen zurückzuführen ist, wie er in den Reaktionsgleichungen [3b] und [3c] dargestellt ist.

Da bei der Bestrahlung von Polyäthylen und Paraffin die gleichen Radikale entstehen (Abb. 3) und auch die Oxydation bestrahlter Proben in beiden Fällen nach der gleichen Kettenreaktion unter Ausbildung von Hydroperoxy-Gruppen abläuft (2), ist ein Einfluß des Molekulargewichts auf die Vorgänge bei der Oxydation nicht anzunehmen. Man wird also die am Paraffin gewonnenen Einzelergebnisse auch zur Erklärung des oxydativen Abbaus von bestrahltem Polyäthylen heranziehen dürfen.

Ich danke Herrn Dr. *G. Müh* und Herrn Dipl.-Phys. *H. Germar* für die Durchführung der Molekulargewichts- und UR-Messungen. Herrn Dr. *U. Johnsen* und Herrn Dr. *H. Fischer* danke ich für eingehende Diskussion, Herrn Professor Dr. *K.-H. Hellwege* für die Förderung der Arbeit.

Zusammenfassung

Durch ESR-Messungen und Bestimmung der Sauerstoffaufnahme wird gezeigt, daß die Oxydation von bestrahltem Paraffin einer Radikalkettenreaktion folgt, bei der Hydroperoxy-Gruppen entstehen. Die Zerfallsprodukte der Hydroperoxy-Gruppen werden durch UR- und Molekulargewichtsuntersuchungen nachgewiesen. Die quantitative Analyse führt zur Aufstellung von Brutto-Reaktionsgleichungen, die den oxydativen Abbau des bestrahlten Paraffins beschreiben.

Summary

ESR investigations and measurements of oxygen consumption show, that the oxidation of irradiated paraffin follows a radical chain reaction which leads to the formation of hydroperoxy groups. The degradation products of the hydroperoxy groups are traced by IR and molecular weight studies. The quantitative analysis results in the formulation of reaction equations which determine the oxidative degradation of the irradiated paraffin.

Schrifttum

1) *Fischer, H., K.-H. Hellwege* und *P. Neudörfl*, J. Polymer Sci. **A 1**, 2109 (1963).
2) *Fischer, H., K.-H. Hellwege, U. Johnsen* und *P. Neudörfl*, Kolloid-Z. u. Z. Polymere **195**, 129 (1964).
3) *Smaller, B.* und *M. S. Matheson*, J. Chem. Phys. **28**, 1169 (1958).
4) *Lawton, E. J., J. S. Balwitt* und *R. S. Powell*, J. Chem. Phys. **33**, 395 (1960).
5) *Loy, B. R.*, J. Polymer Sci. **44**, 341 (1960).
6) *Hawkins, E. G. E.*, Organic Peroxides (London 1961).
7) *Grassie, N.*, Chemistry of High Polymer Degradation Processes (London 1956).
8) *Walling, C.*, Free Radicals in Solution (New York 1957).
9) *Arndt, R. R., J. B. Barbour, E. J. Engels, D. H. S. Horn* und *D. A. Sutton*, J. Chem. Soc. **1959**, 3258.

Anschrift des Verfassers:
Dipl.-Phys. *P. Neudörfl*, Deutsches Kunststoff-Institut
6100 Darmstadt

From the H. H. Wills Physics Laboratory, University of Bristol (England)

Polymer Deformation in Terms of Spherulites

By I. L. Hay and A. Keller

With 43 figures in 77 details

(Received May 12, 1965)

Glossary of Notation in the Figures and in the Text

↑	Draw direction
	With reference to polarising optics
+	Observations made between crossed polaroids. The orientation of the cross gives the polariser and analyser directions in the corresponding photograph. The following two cases are given special notations:
+ ↑ ≡ (||)	Draw direction parallel to the transmission direction of polariser or analyser.
× ↑ ≡ (45)	Draw direction at 45° to transmission direction of polaroids.
	Other cases refer to specified angles between polaroid transmission directions and the draw direction.
($^1/_4\,\lambda$)	Crossed polaroids plus two-quarter wave plates crossed at a right angle and at 45° to the polaroid transmission directions,

one-quarter wave plate being below the other above the specimen.

With reference to spherulite radii

$\parallel$ Spherulite radius parallel to the draw direction

$\perp$ Spherulite radius perpendicular to the draw direction.

$\diagdown$ Spherulite radius oblique to the draw direction.

With reference to index ellipsoids

$1_\parallel$, $1_\perp$, $1_\diagdown$ Long axis of index ellipsoid (chain direction in uniaxial approximation) perpendicular to viewing direction.

$2_\parallel$, $2_\perp$, $2_\diagdown$ Long axis of index ellipsoid (optic axis – coincident with the chain direction in the uniaxial approximation used here) parallel to viewing direction.
In both cases subscripts $\parallel$, $\perp$ and $\diagdown$ refer to the type of radius along which the index ellipsoid is situated.

1. Introduction

It is by now well established that crystalline polymers possess a microstructure on a variety of dimensional levels. It is clear that the existence of these structures must basically affect the traditional conception of deformation in general and fibre formation in particular. This means that the traditional treatment of deformation in amorphous polymers, which is essentially based on reorientation of molecular segments as required by an affine deformation, cannot be directly transferred to crystalline polymers simply by replacing segment orientation by crystallite orientation in proportion to the degree crystallinity. Instead a detailed understanding of the deformation behaviour of the microstructural units is called for the need for which is now gaining recognition. This is indicated by the increasing number of studies on the deformation of spherulites in terms of the microstructure [e. g. *Keith* and *Padden* (1), *Stein* and co-workers (2–4), *Yu* and *Ullman* (5), *Ingram* and *Peterlin* (6), *Cooney* (7), numerous illustrations and comments in the textbook by *Geil* (8), *Barish* (9)] in addition to the earlier sporadic recognition of the fact that spherulites, being part of the material alter their shapes as the sample is deformed as a whole [e. g. *Jenckel* and *Klein* (10), *Bryant* (11), *Langkammerer* and *Catlin* (12), *Hammer* et al. (13)].

The material to be presented here is not the result of one particular investigation it is rather a selection from material accumulated over the past seven years in this laboratory. We tried to select such features which we believe are of general consequence for the subject as a whole. Parts of it are fragmentary to varying extents; it has not been possible to fill some of the gaps at the later stage of writing. The principal aim of the paper is to draw attention to all those factors in deformation which follow directly from the known features of the microstructure, spherulites in particular, through concrete examples. We are aware of the fact that some of the individual features may have been reported elsewhere since the observations, now to be described, were made and further that some features in the literature may be at variance with our findings. However, in view of the complexity of the material it would be difficult to make critical comparisons and it would certainly be exceedingly lengthy to pursue the full bibliography of each feature individually. We therefore have to refer the reader to the references listed collectively and proceed to describe our own material which is selfcontained as it stands. To our knowledge a comprehensive presentation of all the factors to be described here has not been previously attempted.

2. Samples

2.1 General

While making some claim for generality the experiments themselves refer to certain very special circumstances. Firstly, they were all carried out on one specific material: polyethylene. Some features may well be specific to this particular substance. We believe nevertheless that as in the case of single crystal studies, polyethylene is the simplest and most typical representative of long chain compounds. Secondly, the physical form of the samples used is rather specific. This is imposed on us by necessity. The spherulites need to be clearly seen optically, which in itself limits the work to thin films or sections. The latter case is complicated by the fact that sections other than diametral would need to be recognised and evaluated. For this reason the present observations are restricted to thin films, a simplification usually resorted to in work on spherulites. In addition, to be clearly visible, the spherulites need to be of adequate size and well defined. Spherulites satisfying these conditions, however, usually grow at low supercoolings where the resulting crystalline material, as a rule, is not ductile enough for controlled deformation. Polymers which are drawn in the crystalline state in industrial practice are usually microspherulitic but the spherulites cannot be studied individually in any detail. In view of these conflicting requirements the

samples had to be chosen specially for each purpose which incidentally is the accepted tradition of morphological research.

2.2. Preparation methods

The material used was the linear polyethylene Marlex 50. Two kinds of film preparations were used. The one will be referred to as films from O.C.P. (ortho-chloro-phenol), the other as melt cast.

The O.C.P. films were the subjects of most of the light and electron-optical studies. They were obtained by allowing a solution of polyethylene in ortho-chloro-phenol to cool slowly (over 2–3 hours) to room temperature, in which case a coherent skin of polyethylene formed on the top of the liquid. The resulting film proved to be spherulitic with banded spherulites (fig. 1). Less predictably such films could also be obtained from solutions in nitrobenzene. The origin of these films is as follows: in both o-chloro-phenol and nitrobenzene solutions liquid-liquid phase separation occurs as the solution is cooled while still above the polymer melting (dissolution) temperature. The polymer-rich phase, being lighter, spreads on the surface forming the spherulitic skin when crystallisation sets in. Crystallisation in the solvent-rich phase gives rise to a suspension of single crystals and is of no particular interest for the present purpose. It may also contain polymer latex particles originating from the polymer-rich liquid phase which remained dispersed in the form of droplets in the solvent-rich phase following the phase separation.

The 'melt cast' films were principally used for the micro X-ray work to be reported. They were prepared by spreading a solution of polyethylene in xylene on a hot slide at a temperature above 140 °C, i. e. above the melting point of polyethylene and boiling point of xylene. The xylene evaporates rapidly leaving a molten film of polyethylene behind. On cooling the slide to room temperature the film solidifies exhibiting very well defined banded spherulites.

2.3. Stretching experiments

The films from O.C.P. were particularly suited for deformation studies. When dry, the films had the consistency of tissue paper and tore easily. However, while still moist with solvent they were extensible, suitable parts of them to more than 10 times. It was more convenient to dry the films first – after washing with a volatile solvent – and then soak them in oil (microscope immersion oil was suitable) which regenerated the ductility and also provided the best conditions for microscopic viewing. Stretching was carried out by hand while pressing the film to a slide. For stretching at elevated temperatures the slide was heated.

The films were elastic to an appreciable degree, increasingly so at elevated temperatures. If stretched at 60–70 °C the film retracted on release, losing around 75% of the original elongation. For this reason samples stretched in this way were cooled to room temperature while still under tension. In this case, when tension was finally removed the retraction was 25% or less of the total extension. Slow creep could nevertheless take place over a period of days reducing the specimen length somewhat further. When reheated to the original stretching temperature strong further shrinkage set in practically instantaneously. Similarly, very rapid contraction occurred when the deformed specimens were placed in acetone and ethanol. It is noteworthy that these liquids are powerful stress cracking agents.

3. Light optical observations

3.1. Definition of deformation modes and observation conditions

Elongation of the specimens was seen to be accompanied by deformation of the spherulites. It was obvious from the beginning that there was no unique relation between changes in external dimensions and those in internal structure. The same overall elongation could be associated with a variety of structural effects dependent on stretching modes and specimen types.

In an attempt to systematise the variety of effects observed we define two categories. 1. Inhomogeneous and 2. homogeneous deformation. In case 1 the spherulites, or regions between them, yield in one part only which then draws out fully, the rest of the microstructure remaining unaltered. Further stretching occurs by the drawn out regions spreading at the expense of the unaltered portions. In case 2 all parts of a given spherulite extend simultaneously, the extension in different parts thereof being in constant proportion. Most observed cases are intermediate between 1. and 2. To simplify the presentation actual observations will be grouped in one of the two extreme categories whichever they appear to conform to more closely. In general high temperature, while facilitating stretching

favoured 1. and so did increasing sample thickness.

The observations were made under the polarising microscope between crossed polaroids. The photographs reproduced here attempt to convey the main points which were established from many more examples than can be shown. Three principal observation conditions were used. The stretch direction was either parallel or at 45° to the transmission direction of either polariser or analyser. In the third case two quarter wave plates were used, one below and one above the specimen, at right angles to each other and at 45° to the analyser. This latter case corresponds to using circularly polarised light and hence the specimen orientation is immaterial. The three cases will be denoted as (||), (45) and ($^1/_4$ λ) respectively. Photographs of the same areas for all three conditions are shown whenever each has information to add. In addition a few single examples from other sets have been included.

3.2. Inhomogeneous deformations

Two distinct kinds of deformation were observed within this category. In the one the deformation starts within the spherulites, in the other between the spherulites.

3.2.1. Deformation within spherulites

Figs. 2 and 3 are two examples of highly inhomogeneous deformation in two stages of elongation. It is seen that the spherulites yield along the regions where the radii are perpendicular to the draw direction. The two, at first sight, unaffected regions then become separated by highly drawn portions which extinguish in cases (||). On closer inspection, however, changes can also be noticed in the apparently undrawn regions: the dark crosses become zig-zags, particularly pronounced in the (||) position. (In some samples zig-zag extinction lines were already visible within the dark cross in the undeformed starting material. These became more pronounced on deformation.) In the (45) position the zig-zag cross arms rotate slightly towards the draw direction enclosing an angle less than 90°. The discontinuity between the drawn and undrawn (or little affected portions) is apparent in all three [(||), (45) and ($^1/_4$ λ)] settings. The zig-zag and radial extinction lines not visible in the ($^1/_4$ λ) position, a dark and light ring structure, somewhat more widely spaced than originally, however, persists in the undeformed portions. The yielded portions spread through the spherulites at a gradually decreasing rate, as regions where the radii are predominantly parallel to the draw direction are approached. Continued elongation then consists increasingly of the yielded portions pulling out still further. (This can be seen from the thinning of these regions as revealed by the decreasing brightness in spite of improved orientation (fig. 13).)

3.2.2. Deformation between spherulites

In a number of cases yielding set in first between the spherulites at those boundaries which were perpendicular to the draw direction, so that the spherulites themselves became more separated (fig. 4). The spherulites adjacent to these regions may become slightly elongated and reveal a pronounced zig-zag extinction pattern in (||) position. The yielded regions do not seem to sprad readily into the spherulite across the boundary perpendicular to the draw direction, (i. e. along the radii parallel to the draw direction), rather the yielded interspherulitic regions pull out further on increasing elongation. However, when a yield zone meets a spherulite along a boundary which is parallel, that is in a radial region perpendicular to the draw direction, it spreads over the whole spherulite which pulls out inhomogeneously in that region (left side of fig. 4).

Conditions for such interspherulitic deformation were not established except that it occurred under conditions which favoured inhomogeneous deformation of the spherulites themselves. (Effects as in figs. 2–3 and in fig. 4 could be observed in the same sample). Undoubtedly the films were thinner along the spherulite boundaries than elsewhere, noticeable in transmission electron micrographs, which would produce stress concentration there (a factor which would not be at play in case of three dimensional samples). Accordingly we cannot be certain whether this particular effect reflects an intrinsic property or not, and it will not be discussed any further. However, in all the other cases (figs. 2–3, and 5–13) deformation is more pronounced within the spherulites, in spite of the film being thinner at the boundaries and therefore reflects sites of genuine weakness within the spherulites themselves.

3.3. Homogeneous deformation

Figs. 5–12 are illustrations of the predominantly homogeneous deformation in

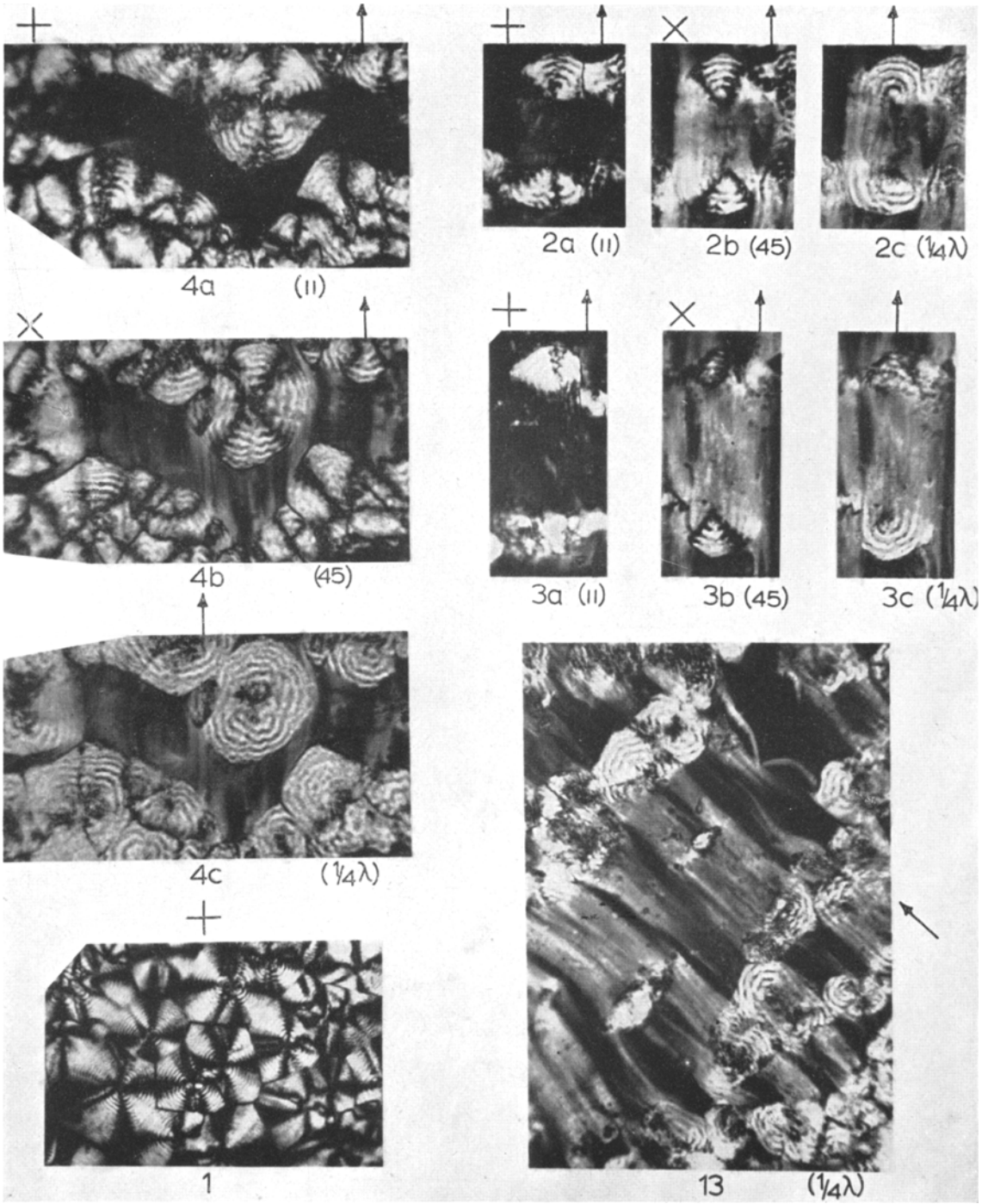

Plate 1. Optical micrographs (for notation see glossary and text. Magnification 185× unless otherwise stated)

Fig. 1. Undrawn O.C.P. film (75×)

Figs. 2 and 3. Two stages of inhomogeneously deformed spherulites

Fig. 4. Drawing at interspherulite boundaries

Fig. 13. Very highly drawn film showing voids with spherulite deformation of the type as in figs. 2 and 3 (150×)

order of increasing elongation. As already stated, most observed cases are intermediate between homogeneous and inhomogeneous. When making the distinction we considered the deformation as belonging to the homogeneous category when under condition (||) an elongated form of the periodically banded spherulite could still be seen, the spherulite being in uniform overall brightness apart from the extinction crosses. This is more or less the case all through figs. 5–12 even for very high deformations as in figs. 11 and 12. It is seen that the cross arm along the draw direction again exhibits a zig-zag (figs. 5a, 6a, 7a, 8a); the overall blackening in the area of the cross arm perpendicular to the draw direction is much more pronounced and obscures details. In the case of the highly elongated samples of fig. 11 two additional photographs are included slightly off the (||) position in either direction. It is seen that for clockwise rotation of the polaroid (fig. 11b) the NW-SE spherulite quadrants become dark and for anticlockwise rotation the NE-SW quadrants (fig. 11c).

In the (45) position the spherulite appearance can be rather similar to that found in the inhomogeneous case. Regions along the radii parallel to the draw direction appear to be distinct and unaffected by the elongation compared with the rest of the spherulite. Within these regions the extinction rings are more pronounced and the regions themselves are bounded by approximately radial extinction lines. On small elongations these regions may extend to the centre even if becoming progressively much narrower there (fig. 5d), but as the spherulite becomes more deformed they gradually shrink to the periphery (figs. 6b, 7b, 8b, 10) until they vanish completely (figs. 11d, 12b). It is to be noted nevertheless that these regions need not represent true discontinuities, and in fact there should be no discontinuity at all if the deformation is purely homogeneous. On the usual test with a first order red plate [e. g. *Keller* (14)] the elongated spherulites are seen as negatively birefringent in the (||) position (quadrants along the fast vibration direction in the plate appear overall orange) and so are the distinct regions along the radii parallel to the draw direction in the (45) position. In this latter case the colour changes to blue, hence the birefringence changes sign by this definition, across the boundary. Under ($^1/_4\ \lambda$) conditions the boundary disappears and the region which previously appeared distinct now merges continuously with the rest of the spherulite (figs. 5e, 6c, 7c) in contrast to the persistence of a discontinuity in the inhomogeneous case. (On occasions some discontinuity may still be observable this we attribute to the presence of an inhomogeneous component in the deformation). As under condition ($^1/_4\ \lambda$) all specimen positions are equivalent we may equally compare the pictures under ($^1/_4\ \lambda$) with those under (||). It is seen that the extinction cross and zig-zag disappears, but the ring structure remains. The blackness in the rings, however, is not as pronounced as in the undeformed starting material. Even so, the rings are in stronger contrast in the radial regions along the draw direction and are distinctly more widely spaced there (figs. 5e, 6c, 7c). At high elongations, when the distinct regions as seen in the (45) position disappear, the ring system becomes practically imperceptible under the ($^1/_4\ \lambda$) conditions (figs. 11e, 12c). It is nevertheless still apparent under the (||) conditions (figs. 11a, 12a).

In fig. 5 two positions intermediate between (||) and (45) are also shown (figs. 5b, 5c) which allows the continuous change between the extinction cross in the (||) case and the appearance of the seemingly distinct region in the (45) position to be followed.

It is to be noted that after the regions seen distinct in the (45) position disappear, the spherulite continues to pull out most near the tips along the parallel radii (figs. 11d, 12b), in contrast to the opposite behaviour in the earlier stages (figs. 5–9). Fig. 10 represents the transition stage between the two (see later).

3.4. Dimensional changes

As the microstructure of drawn specimens was seldom uniform over large enough areas we could not establish precise correlation between macroscopic strain and changes in the internal structure of the spherulites. Here only a few rough guiding figures will be quoted. Spherulite deformations as in figs. 5, 10 and 12 correspond to approximately 1.5–2, 5, 7X or higher sample elongations respectively. In the inhomogeneous case small undeformed remainders of the original spherulites could under circumstances still be detected even at tenfold elongation. In view of the number of parameters, temperature, rate of drawing, specimen thickness, etc., which need to be controlled we did not pursue this numerical assignment any further.

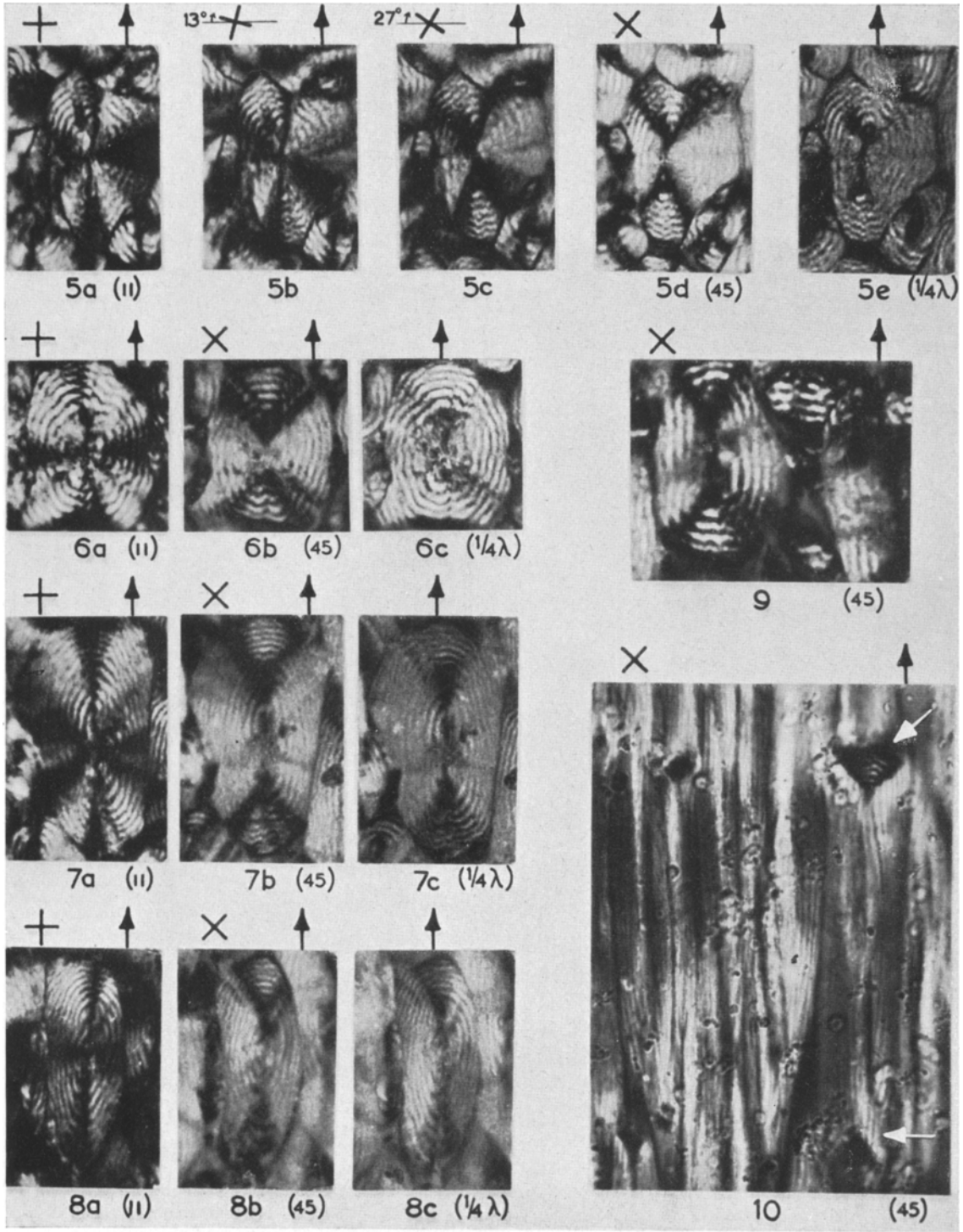

Plate 2. Optical micrographs of homogeneously deformed spherulites (for notation see glossary and text. 275× unless otherwise stated)

Figs. 5 to 8. Spherulites chosen to show progressive stages in the deformation. Fig. 7 is an example of a double spherulite

Fig. 9. Single example of an intermediately deformed spherulite (× 500)

Fig. 10. An example of highly drawn spherulites (see text)

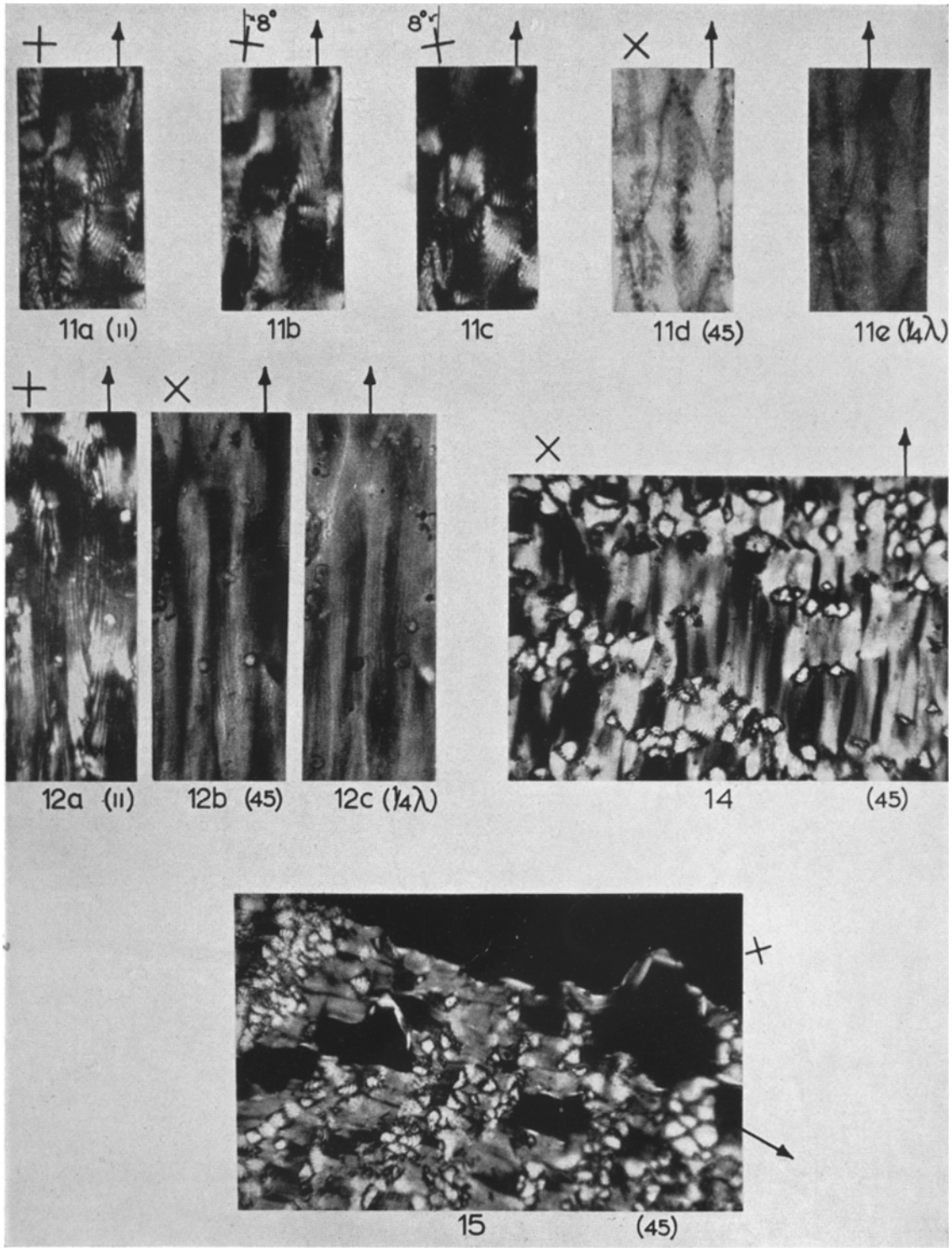

Plate 3. Optical micrographs. (For notation see glossary and text)

Figs. 11 and 12. Strong homogeneous deformation (210×)

Fig. 14. Highly drawn specimen showing void formation (80×)

Fig. 15. Highly drawn specimen showing fibrillation (60×)

As referred to earlier the specimen elongations were to a large extent reversible, partly by spontaneous retraction or creep or, to a much larger extent, through the exposure to heat or to certain immersion media. This was most pronounced with the O.C.P. films. Where in the homogeneous case it was found to be associated with a near complete reconstitution of the spherulite, surprisingly even from states as deformed as in figs. 8–10. This reconstitution occurs by the reversal of the process found on extension. Thus the region appearing distinct along the radii parallel to the draw direction in the (45) position gradually spreads out again until the original spherulitic appearance is attained. The inhomogeneously drawn sample also retracts but the original spherulites are not reconstituted. The yielded regions stay as such but reduced in length revealing a cross striated structure. The reconstitution of the spherulites ceases or is only partial in samples which here we class as homogeneously deformed at elongations exceeding 5× or so. We were unable to define, however, the exact conditions which determine when a spherulite can be reconstituted and when not. It appears that the amount of inhomogeneity present – as defined in the present context – is the controlling factor.

3.5. Observations at very high elongation

3.5.1. Extinction variations

In the case of extreme specimen elongations, 10× or more, the above grouping into homogeneous and inhomogeneous deformations will not be adhered to. In position (‖) complete extinction seems to occur (fig. 16a). However, on rotating the sample slightly off this position in a given direction (say, clockwise) irregular bright and dark bands appear (figs. 16b and 17b). On the same amount of rotation in the opposite direction (anticlockwise) the banded structure appearing is the complement of the one that was seen with the clockwise rotation. The regions which appeared bright before now appear dark and vice versa (figs. 16c and 17a). Comparison of the negatives exposed and processed under identical conditions showed that the most strongly extinguishing regions in the slightly off (‖) position are darker than the overall uniform darkness in the exactly (‖) position. Close examination of the low contrast morphological features revealed some signs of the original spherulitic structure. From these it appears that the regions which in the undrawn state belonged to one spherulite span a dark and light band in the highly drawn state when viewed in off (‖) position (figs. 16b, c). Some fine line structure parallel to the draw direction could also be detected (fig. 17). Summing up, there is a broad irregular periodicity which we associate with the spherulite quadrants (the dark and light regions in figs. 16b and c), and a finer one which seems to be the residues of the ring structure.

3.5.2. Crack formation and fibrillation

Another class of observation in highly drawn samples is the formation of cracks parallel to the draw direction (figs. 13–14) and the eventual splitting of the sample into longitudinal microfibrils (figs. 13, 15). These occur in samples which deformed inhomogeneously, It will be noted that the lateral separation of the cracks and consequently the resulting microfibrils mostly correspond to the width of the deformed spherulites. The cracks develop largely between the deformed spherulites where the boundarie have become parallel to the draw direction. A finer scale fibrillation can also be observed particularly at very high local elongations (fig. 13). This may be related to the original ring periodicity.

3.6. Phenomenological Interpretation of Extinction Patterns

3.6.1. General considerations

In order to aid the discussion, later the extinction effects will be evaluated phenomenologically at this place as a sequel to the observations. At first the principles as laid out earlier by one of us (14) will be recapitulated. Extinction between crossed polaroids can occur for two reasons: firstly, because transmission directions of the birefringent object coincide with those of the polariser and analyser, to be termed zero amplitude effect. These transmission directions are along axes of the ellipse resulting from a section of the index ellipsoid perpendicular to the direction of the light propagation. Secondly, extinction occurs when an optic axis is parallel to the direction of light propagation. This is termed zero birefringence. Here the corresponding section of the index ellipsoid is a circle. When the crossed quarter wave plates are used at 45° to the polaroid direction the zero amplitude effect vanishes but the zero birefringence persists.

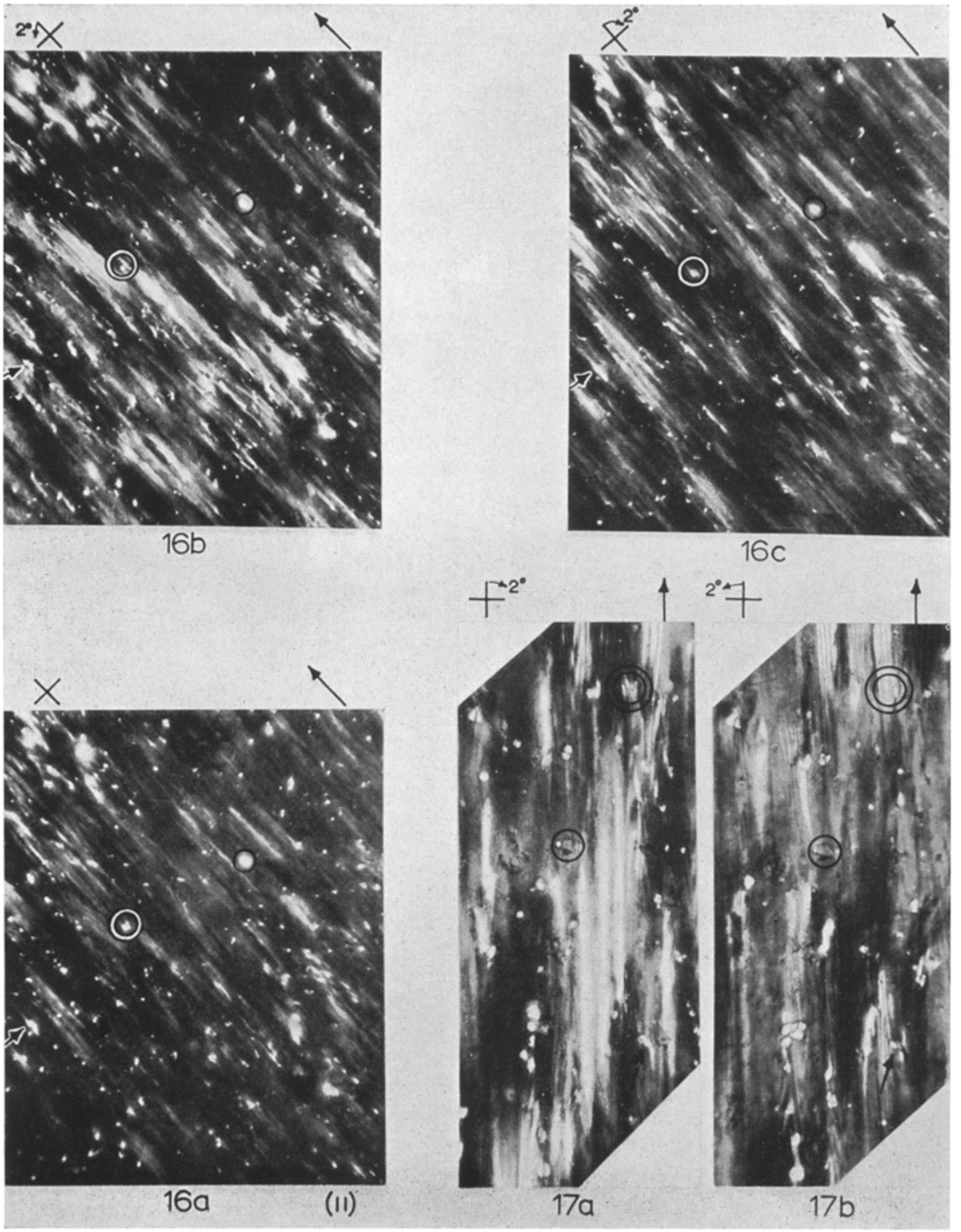

Plate 4. Optical micrographs. (For notation see glossary and text)

Fig. 16. Very highly drawn specimens showing persistence of extinction effects attributable to spherulitic structure. To aid comparison three identical positions are indicated on each photograph. (75×)

Fig. 17. Enlarged area as in fig. 16 also showing the persistence of the fine banded structure. (185×)

3.6.2. Zero amplitude effects

First the zero amplitude effects will be discussed on their own. For this purpose a two dimensional spherulite can be represented as a circularly symmetrical array of index ellipsoids, to a first approximation all being in the same orientation with respect to the specimen plane. Thus they can be represented by identical elliptical sections. As polyethylene spherulites are negative (i. e. direction of maximum polarisability tangential) the long ellipse axes are tangentially oriented. With reference to the radiating morphology this is schematically sketched in fig. 18. (At this stage the variations along a given radius are not represented, the ellipses drawn in fig. 18 could be considered as averages of the variations in fig. 24 to be referred to later). Extinction due to the zero amplitude effect will occur along those radii where the corresponding ellipse axes are parallel to the analyser and polariser transmission directions. These directions are indicated by the cross above each diagram and photograph. In the undeformed spherulite this gives rise to the familiar extinction cross indicated in fig. 18.

Inhomogeneous deformation

Here the final alignment of the ellipses is practically complete in the yielded regions. In the case of yield within the spherulite this state is indicated in the narrowed down region in figs. 19. Complete extinction in the (||) position is expected and in fact observed (figs. 2a, 3a). The rest of the spherulite is drawn as being unaffected.

The boundary creates a special problem. The extreme possibilities are that they lie a) along a radius (fig. 19a or b) along a line normal to the draw direction (fig. 19b) (to be discussed later). In both cases the extinction directions should be at right angles to each other converging towards a point which is reached in a) but not in b). However, observations show that these extinction lines are at variable angles, somewhat less than 90°, and meet at a point which together with the appearance of the zig-zag lines (see later) indicates that some deformation must have occurred also in these regions.

Homogeneous deformation

Observations in the homogeneous case are readily accounted for by the sequence of figs. 20–23. It is obvious that in the (||) position (fig. 20a) there should be extinction along the long and short axes of the elliptically deformed spherulite giving rise to the cross observed. It also follows that a larger region about the short spherulite diameter will appear dark owing to the small orientation changes over a large angular interval which is in accordance with observations. The sequence in figs. 21–23 demonstrates how the distinct regions in position (45) originate and how they gradually contract to the tips until they disappear (fig. 23). The latter effect occurs because the ellipses are nowhere at an angle as large as 45° to the draw direction. The sequence in fig. 20 in combination with fig. 21 shows how the observed transition between the effects in the (||) and (45) arise for a case as in figs. 5a to d. In the case of the highly elongated state of fig. 23 the extinction effects in two positions about the (||) position are indicated, which should explain the origin of observations as in figs. 11b, c, where pairs of diametrally opposed sectors extinguish according to which direction the polaroids are rotated.

It is seen from fig. 22 that there are singular points in the spherulites where the extinction lines meet. (The figure only shows one in the upper spherulite half.) A singularity at the centre is intrinsic to spherulites as for that matter, to any spherically or circularly symmetric structure. In the case of spherulites this difficulty is resolved by the fact that the macroscopic symmetry does not extend to the exact centre when examined with sufficient resolution [*Keller* and *Waring* (15) see later]. In figs. 6–9, however, two singularities appear along the long spherulite diameter equally spaced from the centre. While these can correspond to genuine discontinuities, the material along the long spherulite diameter between these points being much more elongated than elsewhere, this is not a necessary corollary of the extinction pattern as such. As will be apparent, the cusp in the extinction line in itself can be accounted for by a gradually varying orientation within the spherulite.

3.6.3. Zero birefringence effects and the radial periodicity

No attention has been given so far to the radial periodic extinction effects (rings in fig. 1). The origin of these is by now well established [*Keller* (14), *Point* (16)] and worked out in considerable detail (17–20) even if the reason for their existence is not understood. In brief, successive index ellipsoids are regularly rotated with respect to each other when proceeding along a given

radial direction. If the rotation axis is perpendicular to an optic axis (or axes) zero birefringence effects will result at appropriate stages of the winding giving rise to concentric extinction rings, otherwise zero amplitude effects only will arise producing zig-zag distortions of the extinction cross. The contrast effects due to this winding can be observed, even when the zero conditions (in both the amplitude and birefringence case) is not exactly satisfied, provided that there is a sufficient variation in the birefringence and amplitude left. In fact whether the zero condition is reached or not cannot be decided by inspection without tilting experiments and an absolute intensity reference.

For the present it will be assumed that polyethylene is uniaxial. Fig. 24 shows a polyethylene spherulite with the index ellipsoid in two extreme positions: the optic axis parallel and perpendicular to the plane of the spherulite. The former is seen in the projection of maximum ellipticity, the latter with circular cross section (1 and 2 respectively). 2 clearly corresponds to zero birefringence and is responsible for the extinction rings.

In the final orientation when all index ellipsoids are parallel the ring structure disappears. This is the case in the yielded portions of inhomogeneously deformed spherulites (fig. 19) which is in agreement with observation (figs. 2–3). In all other cases the radial periodicity persists to varying extents, which implies that the index ellipsoids have not all become fully parallel along a given radius. The situation is simplest along perpendicular radii. Here, parallel alignment implies rotation of ellipsoids $2_\perp$ into the same orientation as that of $1_\perp$ (and similarly for intermediate cases) about the axes parallel to the radius. Partial alignment implies intermediate amounts of this rotation. Along parallel radii both $1_\parallel$ and $2_\parallel$ (and those in intermediate positions) have to tilt towards the draw direction. The situation is demonstrated schematically by fig. 25. Consider first the perpendicular radii. The alternating initial arrangement in fig. 24 should finally disappear with ellipsoids $2_\perp$ rotating around the radius until their long axes become aligned along the draw direction. In this case the alternation disappears and the ellipses will all be as $1_\perp$, the original $1_\perp$ not being affected at all. Fig. 25 shows an intermediate state with the ellipses having alternating ellipticities. This implies an alternation in birefringence which gives rise to the intensity alternations (but no zero birefringence) observed in all but the extreme elongations. For this latter case, which includes the yielded region of the inhomogeneous deformation, all the ellipses are parallel and therefore in the same orientation with respect to the polaroids. Hence no periodicities are expected from the zero or alternating birefringence or amplitude effect.

In the case of radii parallel to the draw direction all ellipsoids are at right angles to the draw direction in the intial stage thus they should all tilt on drawing. As all initial ellipsoid orientations are equivalent with respect to the draw direction the amount the ellipsoids tilt towards the draw direction should be identical for all (although exact identity is not essential for the argument to follow). This means that they will represent a helicoidal array in which the consecutive ellipsoids are still rotated about the spherulite radius which, in this case, is not at right angle to the ellipsoid axis. Such an array will produce a projection of the type shown by fig. 25, where both the ellipse orientation with respect to the radius and the ellipticity vary periodically. The former can give rise to zero amplitude effects producing zig-zag patterns which are removed under the $(^1/_4\ \lambda)$ viewing condition leaving the birefringence variation reflected by the alternating ellipticity in fig. 25 as the only observable periodicity. This is in complete agreement with the present observations (figs. 2, 5, 6, 7, 8, 11).

In fig. 25 the extinction lines enclosing the apparently distinct region in the (45) condition are also represented. It is seen that along the parallel radii the long of ellipses axes are at angles larger than 45° with respect to the radius within the distinct region (i. e. near the extremities) while this angle is within 45° outside the distinct regions (i. e. near the centre). This implies in the first place that the distinct regions will appear as predominantly negatively birefringent with alternating positively birefringent banding of much weaker birefringence separated by closely spaced extinction lines (due to zero amplitude effect) in the (45) position on the usual test with the first order red plate. The weak and narrow positive bands together with the extinction rings usually appear as a single broad dark band and hence does not affect the overall negative character of the birefringence. All other regions will appear as positively birefringent under the same conditions with no banding or with banding

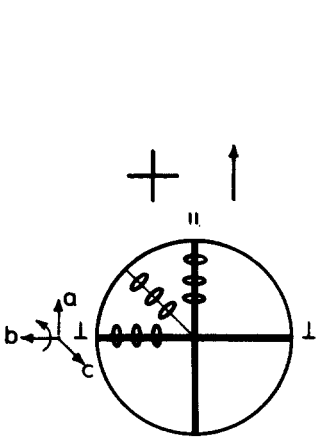

18

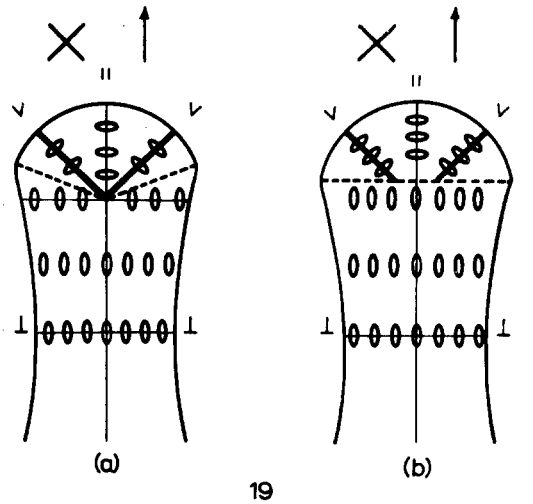

19

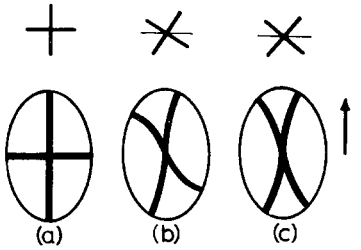

20

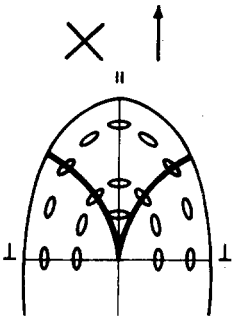

21

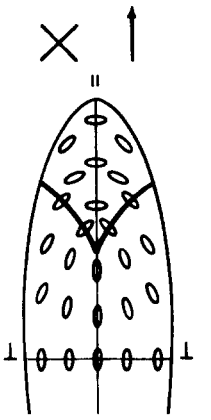

22

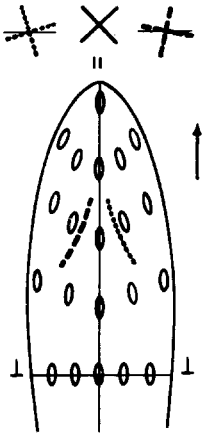

23

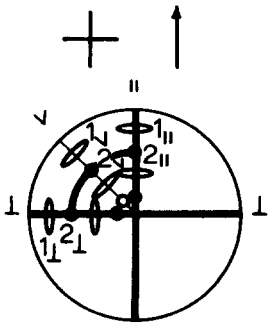

24

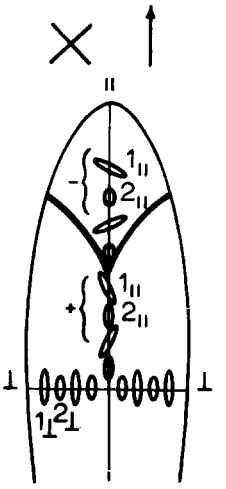

25

Plate 5. Diagrams to illustrate the optical extinction effects. (The extinction loci are indicated by heaviest lines. For notation see glossary and text.)

Fig. 18. Undrawn spherulite. (Averaged index ellipsoid)

Fig. 19. Inhomogeneously deformed spherulite. (Averaged index ellipsoid). a) Radial boundary, b) boundary perpendicular to draw direction

Fig. 20. Variation of extinction brushes with relative orientation of draw direction and polariser

Figs. 21, 22, 23. Successive stages of homogeneous deformation in terms of an averaged index ellipsoid

Figs. 24 and 25. Undrawn and homogeneously deformed spherulites in terms of the periodic radial variation of the index ellipsoid

seen in low contrast only in the (45) position in full agreement with observations. (The two types of regions marked by + and − in fig. 25, are seen as blue and yellow respectively). This scheme implies that the observations can be accounted for without necessarily involving a discontinuity along the parallel radii. Instead it is sufficient to vary the inclination of the ellipsoid axes with respect to the radius continuously along the radius, the long ellipsoid axes becoming increasingly aligned towards the spherulite centre. The extinction cusp will then occur where this angle is 45°. This implies a higher degree of reorientation near the centre, and approximate preservation of the original periodic structure at the periphery with all stages between. Closer observation nevertheless indicates that orientation changes along the radius in some cases can be fairly abrupt (even if this is not a necessary condition for the extinction cusps, as just discussed).

For ellipsoids 2 the long diameter is perpendicular to the draw direction, hence furthest removed from the final orientation equally along all radii. These ellipsoids should all be affected by drawing, hence the zero birefringence effect they are responsible for in the initial stage in the uniaxial approximation should disappear. Indeed observations under the ($^1/_4$ λ) condition reveal a decrease of the contrast between the bright and dark bands, as compared with the initial stage, in agreement with expectations. However, closer observations reveal that this contrast remains stronger along parallel than along perpendicular radii which means that ellipsoids 2 are less affected along the former in spite of the fact that as regards long axis orientation all ellipsoids 2 are indistinguishable.

The situation along intermediate radii would be more complicated to analyse, but the same principles apply. In view of the higher central elongations implied by figs. 42c (see later), an original radial line, other than the ones parallel and perpendicular to the draw direction, will be curved (see fig. 43c). The residual periodicity therefore would have to be traced along such curved lines. This will not be attempted. It should suffice to state that residual periodic orientation variations are observed and the situation is intermediate between those along the two extremes discussed earlier.

3.6.4. Very high elongations

At very high elongations the periodicity is of the zero amplitude type visible under (||) condition, the birefringence variations observed under ($^1/_4$ λ) condition becoming negligible. This situation arises as follows: when the ellipsoid alignment is nearly complete the periodic variation of the ellipticity of the elliptical projections become too small to produce conspicuous contrast effects. Small periodic orientation variations of the ellipses in the plane of the film, however, will produce extinction due to the zero amplitude effect, provided a direction corresponding to extinction is within this range of variation. This condition is clearly satisfied in the (||) position even for highly oriented samples. Here the ellipses are everywhere near final alignment which corresponds to extinction. Small orientation variations are therefore sufficient to produce the effect in question, in agreement with what is observed (figs. 11, 12). Conversely, observations under these conditions usefully serve to reveal residues of the original periodicity at surprisingly high elongations which if it were not for these special observation conditions would pass undetected.

4. X-ray Investigations

4.1. Macro X-rays

Conventional macro X-ray photographs revealed progressive orientation on deformation as expected. In the case of the films from O.C.P., however, the orientation developed more slowly on deformation than is usual in bulk polyethylene. Elongations of 6× and beyond were required for a good fibre pattern with *c* axis (chain) alignment. For lower elongations the usual range of intermediate states of orientation, as established in previous studies on polyethylene, were found (21, 22, 23). Thus the 200 reflexions intensified first on the equator with 110 and 020 reflexions broadly split and contracting gradually on continued elongation (fig. 26, the diffraction patterns were very weak because of the thinness of the films). Diffraction patterns as in fig. 26 corresponded to spherulites as in figs. 8–10.

Occasionally diffraction patterns as in fig. 27 were obtained with sharply contracted hk0 reflexions on the equator superposed on a more or less intense ring or broad arc. The ratio of ring to sharp spot intensity was widely variable. Such patterns correspond to samples with highly inhomogeneously deformed spherulites but no attempt was made to correlate optical image and diffraction pattern with any precision.

When the original spherulites could be reconstituted by relaxation the orientation effects were also removed from the diffraction pattern. Patterns as in fig. 26 randomised along the same route as that by which the orientation became established, i. e. 200 arcs persisted while 110 and 020 arcs became more widely split and spread out. This is in contrast to the familiar relaxation behaviour which consists of 200 arcs splitting first on

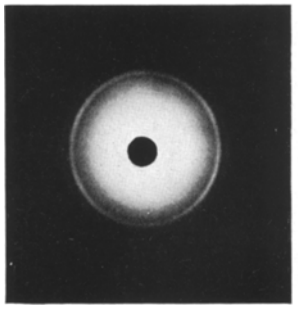

Fig. 26. Macro-X-ray pattern from an intermediately drawn film. (Draw direction vertical)

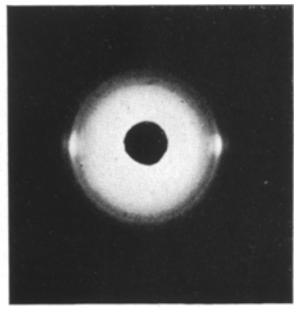

Fig. 27. Macro-X-ray pattern from a highly drawn film. (Draw direction vertical)

Diffraction patterns were taken of several spherulites drawn to varying extents, on several different radial regions. Optical micrographs were taken in each setting while on the X-ray camera which provided records

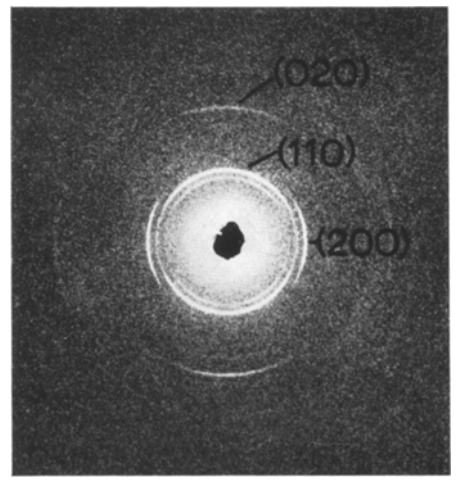

Fig. 28. Micro-X-ray pattern from a radius of an undrawn spherulite. (Radial direction vertical). The principal reflections are indexed, the innermost reflection (not indexed) is due to unfiltered K_β-radiation

retraction (21, 22, 23). However, there were indications of this latter behaviour in very highly drawn samples with pronounced *c* axis alignment.

4.2. Micro X-rays

These examinations were carried out on the melt cast type films, as only these were thick enough to give a pattern within acceptable exposure times. The apparatus used was similar in principle to that described in ref. 24 with some differences in the mechanical construction. Collimation was again achieved with lead glass capillary, the end face of which was coated with gold. This enabled the whole field to be seen in green colour within which the hole could be distinguished as a bright spot when viewed in transmitted light. Viewing was by a polarising microscope attached horizontally to the camera itself. The substance assembly was in front of, the microscope tube behind the capillary and specimen, both being demountable. Punched film was employed thus disposing of the back stop. Specimen plate distance was of the order 3–4 mm, the collimator diameter was variable in general $\sim 20\,\mu$ or somewhat less. Unfiltered CuK radiation was used.

of the exact area selected. Clear distinction between the different phases of the radial windings could not be made with the capillary diameters used. In some photographs, however, the possibility of a marginal selection is indicated (see later). The diffraction pattern of a selected peripheral region of an undrawn spherulite is shown in fig. 28. The principal reflections 110, 200 and 020 are marked on the photograph. The innermost ring is due to CuK_β. Results on drawn spherulites are presented in figs. 29 to 31. In fig. 29 the elongation is slight ($1^1/_2\times$), in fig. 31 it is high ($5\times$), while in fig. 30 it is intermediate rather on the low side ($2\times$). The drawings are accurate reconstructions from the setting photographs. The micro-X-ray work preceded the establishing of the classification by the optical behaviour adhered to throughout this paper, nevertheless it was possible to make an assignment on the basis of the micrographs available. Accordingly the spherulites in figs. 29 and 30 are predominantly homogeneously, while the one in fig. 31 is inhomogeneously deformed. As seen, the final fibre orientation is established in fig. 31 along the radii perpendicular to the draw direction while the original spherulite type orientation

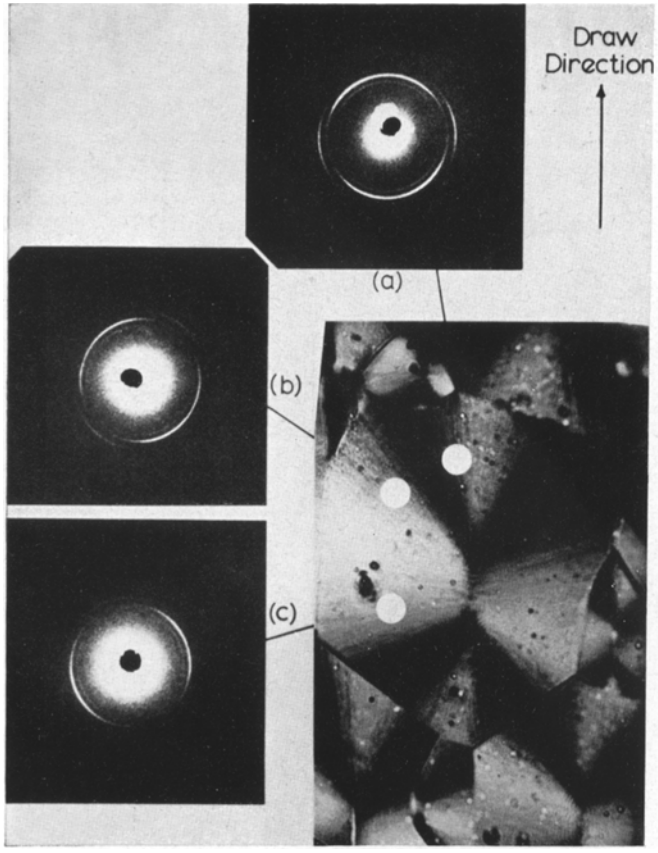

Fig. 29. Micro-X-ray patterns from several areas of a lightly drawn spherulite together with a micrograph of the original spherulite indicating the parts irradiated. (Blemishes retouched)

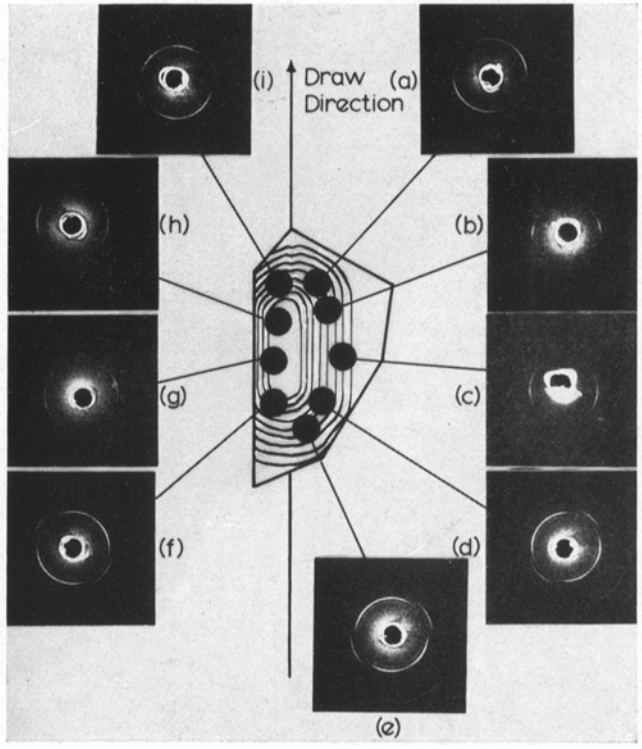

Fig. 30. Micro-X-ray patterns from several areas of a spherulite with intermediate deformation. The line drawing is an accurate reproduction of the original spherulite. (Blemishes retouched)

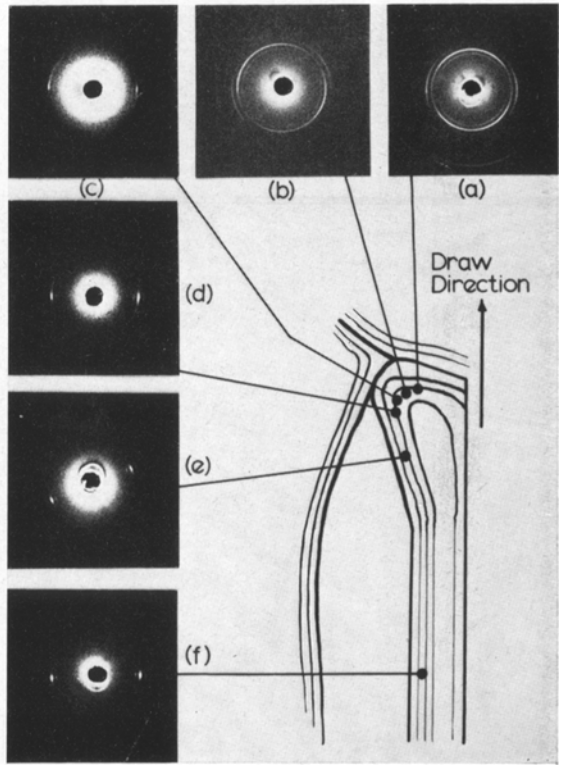

Fig. 31. Micro-X-ray patterns from several areas of a highly deformed spherulite. The line drawing reproduces the boundary of the spherulite accurately – the ring spacing is only schematic. (Blemishes retouched)

with only slight modifications persists along the parallel radii throughout. Various transition stages are observed in the intermediate stages of elongation and along the oblique radii in all stages of elongation. The patterns will be evaluated individually in the discussion.

5. Electron microscopy

These studies are largely fragmentary and only of a supplementary nature. Owing to the thickness of the films replication was required. This was of two kinds – true and detachment replica. The former was carried out by a conventional two stage process with formvar. The latter method consisted of coating the film with carbon and dissolving the material partially in xylene (25). In contrast to the earlier work on single crystals, difficulties were experienced in the dissolution process. The dissolution temperature had to be raised to 115–120 °C and 10–15 minutes exposure to the solvent was required. Backing with silver was required to minimise the breaking up of the film during dissolution. The silver was dissolved subsequently.

The two-stage replicas essentially confirmed the overall picture gained by the light microscope. The ring structure persisted longer along the parallel than along the perpendicular radii, the deformation being more pronounced in the latter region. Fig. 32 illustrates this in the case of a highly deformed spherulite. Amongst the numerous structural features observed (not to be illustrated here) sharp transverse striations will be mentioned seen in highly drawn probably yielded portions.

The detachment replicas were more informative in the present context. The undeformed spherulites showed the radiating twisted structure familiar from earlier work [*Fischer* (20), *Keller* and *Bassett* (26), *Palmer* and *Cobbold* (27)] and will not be illustrated separately. Fig. 33 shows a detachment replica of part of a slightly drawn spherulite, figs. 34 and 35 being details along the parallel and perpendicular radii respectively. This state of elongation corresponds approximately to that in figs. 6–7 amongst the optical micrographs and the corresponding features, namely more pronounced drawing out along the perpendicular radii and wider ring separation along the parallel radii, are noticeable. In addition there is a confused disrupted region in the centre. These and other points will be further commented on later.

Fig. 32. Highly drawn O.C.P. film. Electron micrograph of two stage replica. (Draw direction vertical)

Fig. 33. Lightly drawn O.C.P. film. Electron micrograph of detachment replica. (Draw direction vertical)

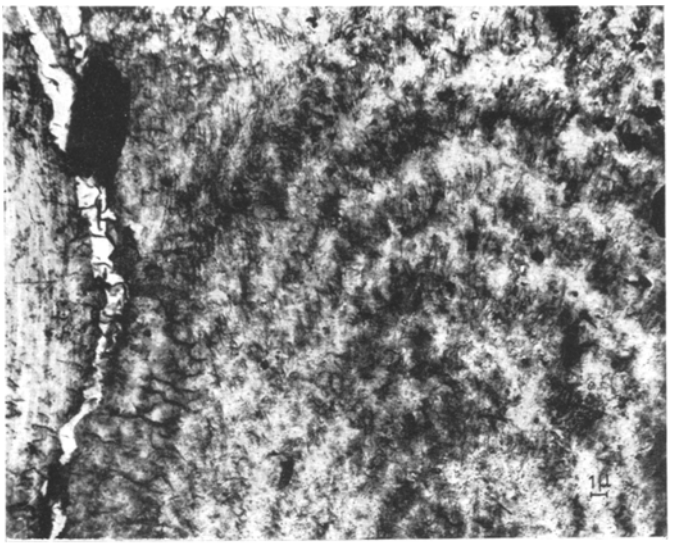

Fig. 34. Enlarged detail of spherulite in fig. 33 showing radii parallel to draw direction. (Vertical)

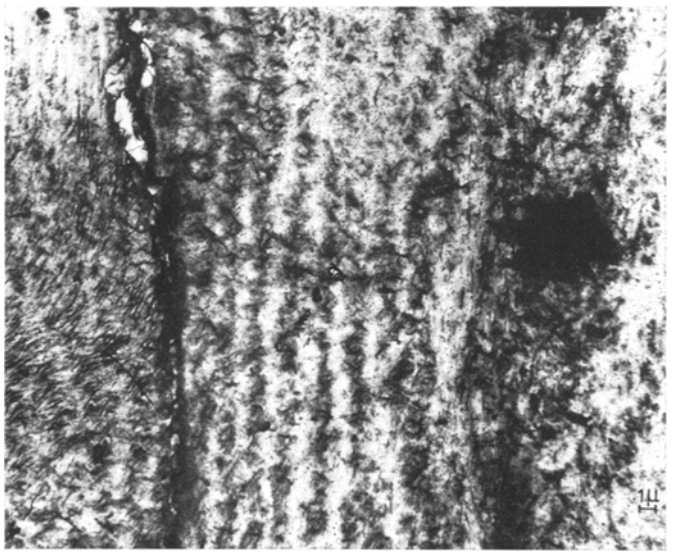

Fig. 35. Enlarged detail of spherulite in fig. 33 showing radii perpendicular to draw direction. (Vertical)

On further elongation features as in fig. 35 spread over most of the sample with the structural features (the dark transverse striations) becoming increasingly pulled out. Completely smooth structures were not obtained even at the highest elongations, some of the dark transverse striations still persisting to varying extents (figs. 36a, b). In the most highly elongated samples, however, the corresponding two-stage replicas were smooth, from which we conclude that in these cases the cross striations were produced by preparation conditions. In fact it was found that the formation of such striations can be promoted by annealing of highly drawn smooth specimens. It appears therefore that some involuntary annealing has occurred during the dissolution process when preparing the detachment replicas of samples which were most highly drawn. For this reason we do not consider effects as in figs. 33–36 as spurious because they correspond to a genuine state of matter characterising both the partially drawn out and the partially retracted state. (This point has already been made in ref. 28 where these same specimens were utilised for low angle electron diffraction reported there).

Detachment replicas are intrinsically capable of producing electron diffraction patterns. Figs. 37a and b are two patterns from undeformed spherulites, one of an O.C.P., the other of a melt cast film. As seen in essence they agree with the micro beam X-ray photograph of fig. 28, except that the 200 reflections are noticeably weaker

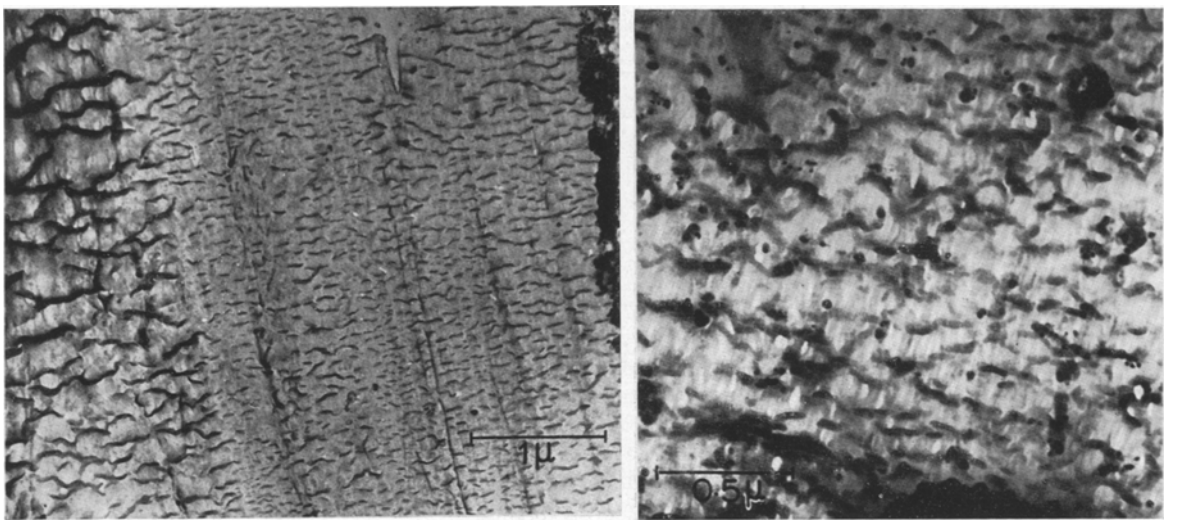

a) b)

Fig. 36. Highly drawn O.C.P. film. Electron micrographs of detachment replicas. Draw direction approximately vertical. [After *Bassett* and *Keller* (28)]

particularly in fig. 37b. Tilting of the samples along a direction parallel to the corresponding spherulite radius was observed to lead to an intensification of the 200 arcs followed by a splitting and subsequent movement of the arcs towards the tilt axis. This is in accordance with expectations if there were no complete fibre symmetry drawn specimens gave the familiar diffraction of a well oriented film (fig. 38). It is essentially identical to the X-ray photographs of the original film from which the detachment replica was prepared. As commented on elsewhere (28) the same highly oriented pattern was obtained irrespective of the amount of cross striation present resulting

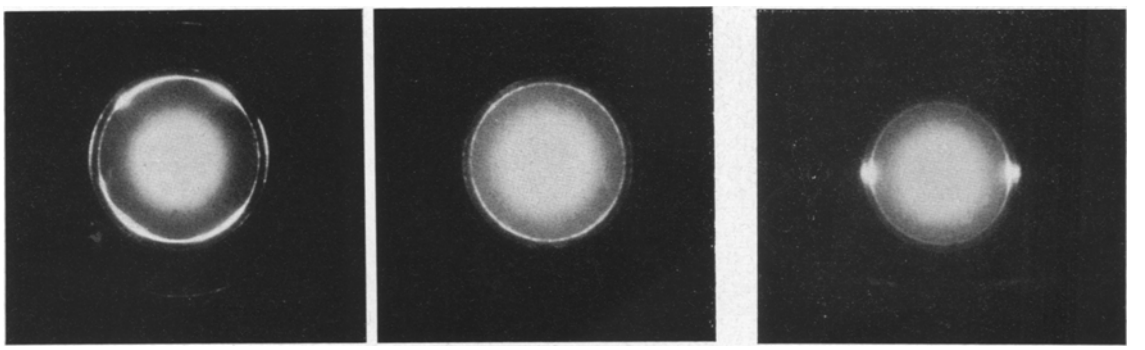

a) b)

Fig. 37. Electron diffraction patterns from detachment replicas of a) Undrawn O.C.P. film. b) Undrawn melt cast film. (Spherulite radius vertical)

Fig. 38. Electron diffraction patterns from detachment replica of highly drawn O.C.P. film. Draw direction vertical. [After *Bassett* and *Keller* (28)]

around the spherulite radius. Then the mean direction of the *a* axis is at an angle to the film plane [see *Keller* and *Sawada* (29)], this angle being given by the specimen tilt where maximum intensification of the 200 ring perpendicular to the tilt axis occurs. This angle was will defined in the very few specimens available. It can only be said that it appeared to be between 10 and 30°. Highly from intentional or involuntary annealing. Intermediate stages of elongation were not examined systematically as regards detachment replica electron diffraction. Technical difficulties in both preparing the samples and in taking the diffraction patterns are appreciable. Undoubtedly much further information could be gained by such examinations.

6. Discussion

The salient point of our observations is that spherulites do not deform affinely in relation to the sample as a whole. This fact has already been more or less explicitly implied in the works referred to in the Introduction (1–9). Thus there are references to different degrees of deformation along the different radii (2–4), to preferred yielding along the perpendicular radii (1), to the partial preservation of the ring structure (8), to periodically varying splitting behaviour across the ring structure (30), to diffraction effects associated with the lamellar texture (6) and to a variety of deformation effects as observed with the electron microscope (8). At this place we shall attempt to lay out the factors at play systematically, backed by the observations presented here.

The changes produced by the elongation are of two kinds: changes in the orientation of the molecules and crystallites, and those in the dimensions of the microstructural units (spherulites). Obviously the two must be related, but as it emerges from our work this relation is not a simple one. First, we shall consider these two aspects individually and begin with the orientation effects without regard to the dimensional changes with which they may be associated. Some comments on the correlations between orientational and dimensional changes will be made at the end.

6.1. Crystallographic orientation effects

6.1.1. General considerations

The average overall molecular orientation in a spherulitic sample is complete randomness; in the highly drawn material the chains or segments thereof are parallel, aligned in the draw direction. In the final analysis this transformation has to be accounted for. We shall follow this transition in terms of what is known about the structure of the spherulite. As the crystal orientation alone is known this will be done in crystallographic terms only: portions of the material not in the form of crystals will not be included in the argument immediately to follow. The discussion will further be restricted to two dimensional spherulites, the subject of our experimental material.

The spherulites are radiating aggregates of crystals. Polyethylene is orthorhombic [*Bunn* (31)] with one of the axes (*c*) parallel and the other two (*a* and *b*) perpendicular to the molecular chains. The *b* axis is radial in the spherulites [*Keller* (22)] which implies a tangential chain orientation. The crystal orientation varies periodically along a given radius – with the crystals arranged in a helicoidal fashion rotating around *b* [figs. 18, 24, and pole fig. 39 (i)]. Although the crystals are strictly speaking optically biaxial we can take them as uniaxial to a sufficiently good approximation with *c* as the optic axis. (Large ellipse diameter in fig. 24).

We consider that the effect of the applied stress is to align the *c* axes in the draw direction. (Should there be competing trends of other crystal directions to become aligned [*Frank, Keller* and *O'Connor* (32)] this would partially modify the considerations which follow). In the different spherulite portions, the *c* axes have different initial orientations with respect to the draw direction, hence the orientation process itself must vary from one locality to the other. These variations will be of two kinds a) from one radius to the other as the inclination of the different radii to the draw direction is variable, b) between the different portions of a given radius in view of the varying crystal orientations along it. One may consider crystal reorientation as occurring by rotation of individual crystals without any plastic deformation or by shear involving more or less uniform slip within the crystals or by a combination of both. Whichever the case, final *c* axis alignment must result which, in terms of the microstructure, can be considered as follows.

6.1.2. Radius parallel to draw direction

Here *c* is always perpendicular to the draw direction while *b* is along it [pole fig. 39 (i)]. Hence crystals in all phases of winding are equivalent as regards drawing. Alignment of *c* must involve a rotation of the unit cell around *a* for all crystals along this radius. Hence either the crystal rotates around *a* as a whole or in the case of plastic deformation must deform by [001] (010) slip. The pole figures in fig. 39 (ii) and (iii) show this reorientation for two crystal positions with *a* perpendicular and parallel to the plane of the paper respectively (position $1_{\parallel}$ and $2_{\parallel}$ in fig. 24). Considering also crystals in intermediate positions it will be obvious that the resulting final orientation will have full fibre symmetry around *c* [pole fig. 39 (iv)].

6.1.3. Radius perpendicular to draw direction [pole fig. 40 (i)]

Here the *c* axis orientation is varying periodically with respect to the draw

direction. In one particular phase of this periodicity the *c* axes are along the draw direction to begin with and do not require reorientation is represented by pole figure 40 (iii). The final orientation for the whole radius is shown by fig. 40 (iv). It will be seen

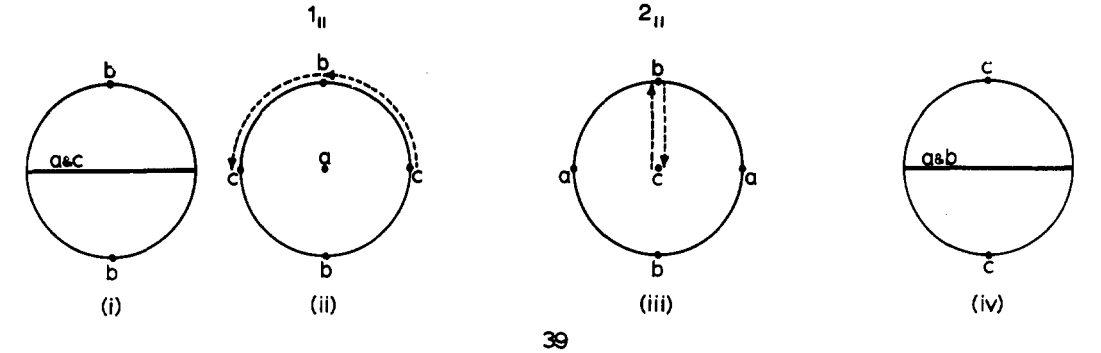

Fig. 39. For radii parallel to the draw direction

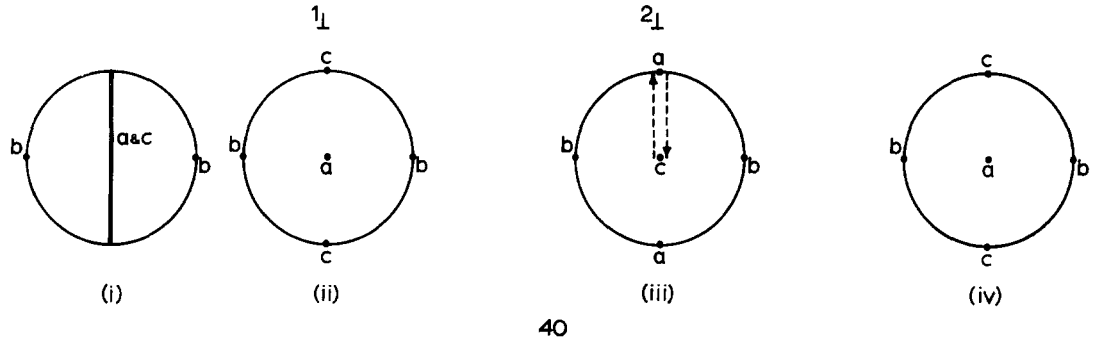

Fig. 40. For radii perpendicular to the draw direction

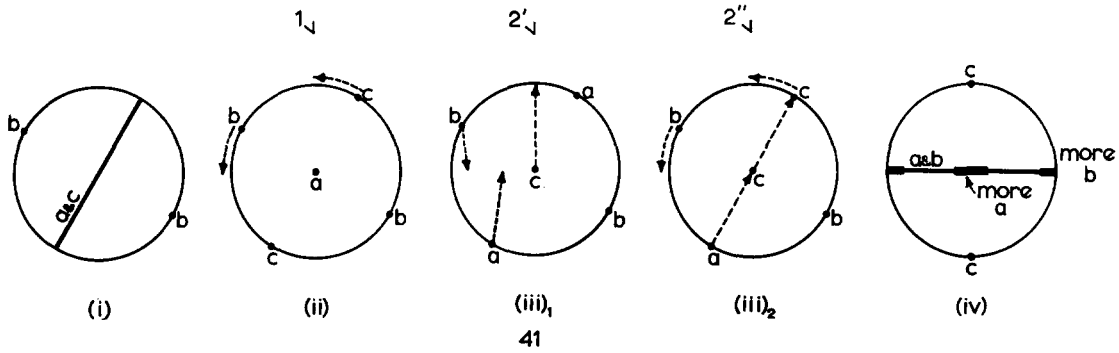

Fig. 41. For an oblique radius

Figs. 39–41. Pole figures illustrating reorientation. (Draw direction vertical)

reorientation [$1_\perp$ in fig. 24, and pole fig. 40 (ii)]. With all other crystals the unit cell needs rotating around *b* by amounts varying between 0° and 90°. The maximum 90° rotation is required for crystals in position $2_\perp$ in fig. 24, and the corresponding that this corresponds to a single crystal with *a* normal to the spherulite plane and *c* along the draw direction. The above orientation process can be achieved either by crystals rotating as such around *b* or by shear involving [001] (100) slip. It is to be noted

that the crystals are lamellae with oblique $\{h0l\}_s$ basal planes [either $\{101\}_s$ or $\{201\}_s$ (*Keller* and *Sawada* 29). The subscript s refers to the subcell; for notation see ref. 33]. This raises the possibility of slip occurring between lamellae with lamellar interfaces as slip planes in addition to or instead of slip within the lamellae. Indeed evidence for interlamellar slip has been found in compression (*Hay*, *Kawai* and *Keller* 39). $\{h0l\}_s$ lamellar interfaces as slip planes could in fact favour c axis alignment along the perpendicular radii, as [001] $\{h0l\}_s$ slip would involve rotation around b.

The existence of interlamellar slip implies that only loose connections can exist between the lamellae, as it requires slip across the chains. This, in turn, implies that a given molecule is largely confined to within a given lamella which is seems to require the presence of appreciable amounts of chain folding.

6.1.4. Oblique radii [pole fig. 41 (i)]

The situation in this case is more complicated. To bring the c axis into its final alignment the unit cell needs rotating around an axis intermediate between a and b. In addition there is no unique direct rotation axis along a given radius; it will be different in the different stages of winding of the crystals along the particular radius. Also it is very likely that rotation does not proceed along the shortest route but is restricted to paths which conform to the requirements of the crystal structure, e. g. by slip modes determined by the lamellar structure (true cell) and chain packing (subcell). Say, for simplicity, that only reorientations which correspond to rotation around a and b occur. At any rate we know from the preceding cases that such rotations must at least be possible. Then the final c orientation could establish itself by these rotations occurring consecutively[1]).

Rotations not being commutative the final orientation about c must depend on the actual sequence. The simplest assumption is that the rotation sequence is determined by the shortest route. For crystals in position $1_\searrow$ (fig. 24) the shortest route is by rotation around a [fig. 41 (ii)]. The shortest route for crystals $2_\searrow$ is shown by fig. 41 $(iii)_1$. Fig. 41 $(iii)_2$. shows the reorientation of crystals $2_\searrow$ by another route, namely consecutive rotations around b and a. We see that the end state will be different for the two cases and, in general, will depend on the route taken. In any case it is expected that the resultant for the whole radius will be intermediate between those in figs. 39 (iv) and 40 (iv) and fig. 41 (iv) has been drawn accordingly. A more precise discussion would be further complicated by the fact that a given radial line in an original spherulite will change its direction and may become curved as the spherulite deforms. (Fig. 43, see later.)

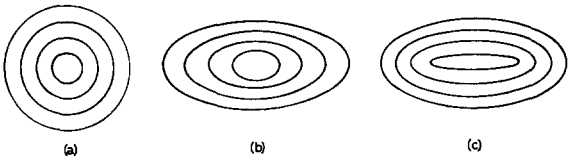

42

Fig. 42. Deformation modes within a spherulite. (Draw direction horizontal). a) Initial spherulite subdivided into spherical shells. b) Affine deformation; shapes of all ellipsoidal surfaces are similar. c) Spherulite deformed to same external shape as (b), but thickness of an elemental shell is uniform. [After *Wilchinsky* (37)]

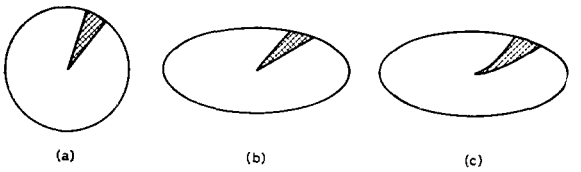

43

Fig. 43. Deformation of a radial sector within in a spherulite. (Draw direction horizontal). a) Before deformation. b) After affine deformation. c) After deformation by mode of fig. 42c. (After *Wilchinsky*)

In conclusion it follows that while the final orientation will correspond to the c axis lying along the draw direction the distribution around c will be different in regions corresponding to different portions of the original spherulite. Full fibre orientation occurs on parallel radii, single crystal orientation for perpendicular radii with a normal to the film plane, and varying intermediate orientation over the rest of the spherulite, dependent on the radius involved and on the exact route taken by the reorientation.

6.2. Comparison with experiment

Some of the observations will be reexamined in the light of the preceding general considerations.

[1]) By the term 'rotation' we wish to signify the reorientation of the crystal axes, without implying that this occurs by bodily rotation of the crystal as a whole. When this latter is intended this will be stated explicitly.

6.2.1. Optical observations

It is clear from the observations that *c* axis alignment occurs more readily along a perpendicular than along a parallel radius. In all cases the original spherulite appearance is more closely retained along the parallel radii – or at least along their outer portions. Here the sign of birefringence remains negative with respect to the draw direction. In contrast to the outer portion of the radii – which for not too high a elongation comprises the larger part of the spherulites – the near central region of the parallel radii elongate drastically with pronounced *c* orientation. In the first place this is a dimensional requirement, as the high elongation along the perpendicular and low elongation along the parallel radii would not be compatible otherwise.

This problem will be touched upon later. It should suffice to state here that in a complex inhomogeneous system where both stress and strain are non-uniform on the micro-scale the high central elongation of the parallel radii need not conflict with the general impression of the parallel radii being less deformable as high local stresses there could be expected. Figs. 10, 11 and 12 nevertheless reveal that deformation can be very pronounced along the parallel radii, even at the outer portions, as seen from the pointedness of the spherulite tips. This is characteristic of the high state of elongation where the distinct regions, as revealed in the (45) position, have already disappeared, which means that the index ellipsoids are all at angles smaller than 45° with respect to the draw direction (fig. 23). Where the distinct regions are still visible, as in the spherulite marked by arrow in fig. 10, the spherulite extremities are broad, consistent with the closer preservation of the original spherulite structure in that locality. It appears therefore that the parallel radii are more resistant to deformation to begin with, but once a certain reorientation is reached – *c* axis alignment closer than 45° – they become readily deformable (whether more highly deformable than elsewhere is not readily assessable from the evidence available). The transition from the first state to the second may well occur discontinuously (yielding) where this yield point travels along the parallel radius. However, as pointed out earlier, the discontinuity, as seen in (45) position, in *itself* does not necessarily imply this. Fig. 10 is particularly revealing as the pointed and the broad tipped spherulites with distinct regions are seen side by side. This demonstrates that it is not the sample type but the state of elongation which is responsible for the different behaviour of the parallel radii.

In what follows we shall concentrate on the first of the two stages i. e. where the parallel radii are least affected, the effect most apparent from our experimental material. As seen from the pole figures in fig. 39 and 40 the orientation along the perpendicular radii in the undeformed spherulite is closer to the final *c* axis alignment, than that along a parallel radius as only crystals 2 and not 1 need reorienting (considering the two extreme crystal orientations). It could be argued that the more complete reorientation along the perpendicular radii is attributable to this. Nevertheless, it follows from the observations that even when those crystals are compared along the parallel and perpendicular radii which have identical *c* axis orientation with respect to the draw direction, those along the parallel radii orient to a lesser extent. The argument is as follows: Consider the observations under ($^1/_4$ λ) condition, when the alternation of dark and light is due to birefringence differences alone. In the initial stage the contrast difference between $1_\perp$ and $2_\perp$ and that between $1_\parallel$ and $2_\parallel$ is the maximum obtainable (complete extinction for $2_\perp$ and $2_\parallel$) and is equal along all radii. On drawing, crystals $1_\perp$ and $1_\parallel$ will both retain their orientation with respect to the plane of the film (i. e. *c* will remain in this plane) and consequently will be of equal brightness, as seen under ($^1/_4$ λ) condition. Hence if there is any difference in the periodic contrast variations along the different radii this must be due to orientation differences in crystals 2 where initially *c* was perpendicular to the draw direction along all radii. In fact it is observed that the rings are in most pronounced contrast along the parallel radii (figs. 5e, 6c, 7c, 8c) which means that of all crystals in position 2 crystals $2_\parallel$ must have been removed least from their initial extinction position. Hence crystals $2_\perp$ and $2_\parallel$ are not equivalent as regards reorientation in the draw direction.

We conclude therefore that rotation of the crystal axes around *b* occurs more readily than around *a*. This may be due to crystallographic factors such as an easier [001] (100) than [001] (010) slip within the lamellae and/or [001] lamellar slip occurring most readily on $\{h0l\}_s$ lamellar interfaces. Indeed

the preference for (100) as slip plane has been noted earlier in connection with rolling unaxially oriented specimens. [*Frank, Keller* and *O'Connor* (32)] and the lamellar interfaces are known to be predominantly {101} or {201} (29). Further, the crystals are twisted around the radial *b* axis direction within the original spherulites which displays a spontaneous trend of crystal rotation around *b* during growth, a trend which is expected to prevail also under an external orienting influence.

We may assume that the above deductions also apply to oblique radii. This would mean that there should be a larger component of rotation around *b* than that corresponding to the shortest route or even for the shortest *b* plus *a* rotation combination (fig. 41). The preference for rotation around *b* could be considered as crystals rotating mainly around the appropriate radial directions first and only then brought into final *c* alignment by rotation around *a*. Some diffraction evidence for this will be given below.

While discussing optical properties it may be opportune to stress a general point which should now be self evident. Correlation of birefringence, as measured on a macroscopic sample, with structural processes occurring during deformation has been standard practice for a long time. It has already been noted that in crystalline polymers at least, there need not be a unique relation between the overall birefringence and elongation. Thus birefringence may decrease and even reverse its sign during early stages of elongation (see e. g. ref. 4). Clearly when the sample is spherulitic and the spherulites are not, or cannot, be resolved individually an average of effects such as described here will be observed. It is obvious that structural features such as presented here are not likely to be deduced from such averages, without independent information on the microstructure as already implied by *Stein* and coworkers (2, 4).

6.2.2. Micro X-rays

It needs to be appreciated that single photographs are inadequate for defining the orientation completely unless information is available on the symmetry independently. The fibre symmetry with respect to the spherulite radii can be taken for granted in the undeformed spherulite (fig. 28) but not after deformation. In these cases complete exploration of the texture pattern is required which would be very difficult with the micro photographs in question. Certain broad conclusions nevertheless can be drawn from the absence or presence of reflections and from their azimuthal positions in the single photographs taken in the course of the present work. On the whole these conclusions tie up very well with the deductions from the optical observations. Fig. 28 is in full accord with the well established radial *b* axis orientation in the undrawn spherulite. This orientation is essentially preserved along the parallel radii in the drawn spherulites (figs. 29a, 30e, 31a).

Taking figs. 29–31 individually, we see that the first sign of change is along the perpendicular radii of fig. 29c in the form of the weakening of the 200 arc. This is consistent with the picture of crystals $2_\perp$ starting to rotate around *b* as in the pole figure of fig. 40 (iii) towards the final position in fig. 40 (iv). There is no noticeable effect along the parallel radii (fig. 29a).

More pronounced changes are seen in fig. 30. The two reflections in the regions of perpendicular radii are 110 and they are in their final position with respect to the draw direction (compare with figs. 27, 38). This would be expected in the case of the final single crystal type orientation as in fig. 40 (iv) with sufficient spread to bring the {110} planes into reflecting position. The conspicous absence of 200 is in agreement with this deduction. In patterns from regions slightly off the perpendicular radius the bisector of the two 110 arcs is tilted with respect to the draw direction and this tilt is in the opposite sense in adjacent spherulite quadrants (e. g. figs. 30 g, 30 h). This is fully consistent with the optical observations as in fig. 11b and c and accounted for by the sketch in fig. 23, where pairs of quadrants extinguish when rotated slightly from the (||) position, different diametral pairs extinguishing for opposed rotation directions. It appears that rotation around the radius (*b* axis) is practically complete leading to the state as in fig. 40 (iv) with the *c* axes all in the film plane, but not yet fully parallel to the draw direction. The same point is even more apparent for the oblique radii closer to the draw direction (fig. 30a). Here the pattern is practically the unaltered spherulite pattern of fig. 28, with the bisector of the 110 arcs lying approximately along the radius, except that the 200 reflections are considerably weakened. This again is indicative of rotation around *b*, as in fig. 41 $(iii)_2$,

with little or no rotation component around *a*. Thus again it appears that the initial rotation of the crystal axes around *b* is preferred to the shortest routes in case of oblique radii. No photograph of a parallel radius is available for this particular spherulite, but considering the diffraction pattern given by the much more highly elongated state in fig. 31a the preservation of the unaltered spherulitic pattern there is expected. The asymmetric pattern of fig. 30b cannot be unambiguously accounted for from one photograph. It could arise if there were a periodic oscillation of the orientation around the radius (remnant of the ring structure) and the collimator did not comprise a full period. Alternatively it could be produced by an unequal spread of the final orientation shown by fig. 40 (iv) about the mean position. This would occur if position (iv) in fig. 40 were approached more from one direction than from the other i. e. by rotation predominantly in one sense. It would not be profitable to elaborate this point on the basis of the evidence available but obviously possibilities such as a connection between the sense of asymmetry in the pattern and the sense of winding along the spherulite radius and possibly the direction of molecular obliquity come to mind.

In the most highly drawn spherulite (fig. 31) these are signs of the full fibre pattern (110 plus 200 reflexion) along the perpendicular radius. Clearly the direct relation to the original spherulite as embodied by fig. 40 is lost. This may well be a general attribute of the yielding occurring in the inhomogeneous spherulite deformation and must be accompanied by a removal of the original spherulitic memory. There is no direct crystallographic reason why randomisation of the texture in fig. 40 should occur around the *c* axis. The strong innermost reflection in fig. 31f is unikely due to CuK_β radiation alone, it is likely to be intensified by the second triclinic crystal modification of polyethylene [e. g. *Turner–Jones* (34)] which is known to occur on deformation [*Frank, Keller* and *O'Connor* (32), *Geil* (35)]. Orientation along the parallel radii, while essentially as in the unaltered spherulite, shows an asymmetry of the 020 with regard to the 200 and 110 arcs. The fact that 020 is not exactly along the draw direction would be a consequence of a slight *c* axis alignment towards the draw direction according to fig. 39 (ii). In this case, however, the 020 should have four components slightly split about the draw direction. It appears that only one diametrally opposed pair of maxima is present. This would arise if the area selected did not comprise a full radial winding period (two extinction rings) in which case only one portion of the full fibre pattern would be produced. Accordingly fig. 31a would be an example where a portion of the radial periodicity is individually resolved. In view of the widening of the ring structure along the parallel radii this may just be possible with the collimators used. The small *c* acis alignment implied would cause the observed zig-zag extinction pattern in accordance with fig. 25. A characteristic asymmetry of the 110 arcs appears in patterns along oblique radii (fig. 31c, d). It can be shown that this follows readily from the underlying geometry. In brief, the 110 arcs are split about the radial direction in the undeformed spherulite. In the final orientation they contract to a pair of arcs lying normal to the draw direction. For a large range of oblique radii this final position of the reflections will be approached from one side only the reorientation occuring along the shortest route. This will lead to the observed asymmetric concentration of intensity. Fig. 31d is intermediate between figs. 31e and 31c and begins to show the asymmetric intensity distribution of the 110 arcs. The area selected was near the yield boundary and we think that the presence of the 200 and symmetric portions of the 110 arcs are due to the yielded portion within the area contributing to the pattern. It will be obvious that the preferential rotation around *b* in the case of these oblique radii is not as prominent here as it was in fig. 30. It appears that in the inhomogeneously deformed sample the *c* axis approaches its final orientation more directly along the shortest route [fig. 41 $(iii)_1$].

6.2.3. Macro X-rays

It will be evident that the usual X-ray photograph taken with a collimator large compared with a spherulite and on a thick sample where the beam traverses many spherulites, the average of all the effects described here will be obtained as in figs. 26 to 27. It would be unprofitable to attempt to account for such patterns in terms of a single process occurring during orientation. The resultant effect would rather need to be

pieced together from that given by the microscopic regions as just discussed[1]).

6.2.4. Electron diffraction

Diffraction patterns in fig. 37a and b will be briefly commented on. Correspondence with the X-ray photograph, fig. 28, is self-evident. The reduced intensity of the 200 reflection, particularly in fig. 37b has already been mentioned. We interpret this as follows. Those layers along the winding radii which are in the flat-on position with respect to the film plane have been preferentially detached, and contribute more to the diffraction pattern. As the molecules are oblique with respect to the layer surface, and this obliquity corresponds to a rotation around *b* ($\{h0l\}_s$ layer surface) the lamellae when viewed flat on will not contribute to the 200 reflexion. *Keller* and *Sawada* (29) found that the obliquity is either 18° ($\{101\}_s$) or 34° ($\{201\}_s$) according to whether the crystallisation temperature is low or high respectively. According to the tilting experiment, the obliquity is less than 30° and may not exceed 20°. This would point to the $\{101\}_s$ alternative. As the samples in question crystallised during comparatively rapid cooling this result is in agreement with expectations.

6.3. Dimensional changes

Changes in crystal orientation are coupled with changes in dimension. We do not know the exact relation between the two – if a unique relation exists at all (see later) – but only that, in general, greater deformations are associated with a better alignment of the *c* axes in the draw direction.

We shall regard the spherulites as isolated and first consider the simplest mode of deformation where each portion of a spherulite extends in an identical manner. The situation can be represented by drawing a circle on a rubber sheet which is then extended. The circle will change into an ellipse in an affine manner. This is one of the two situations discussed lately by *Wilchinsky* (37) who considered the affine deformation of a set of concentric circles (fig. 42). The circles, all except the outer boundary, were considered as hypothetical, serving merely as a 'bookkeeping' device. We now see that they can have physical reality in the form of the directly observable radial periodicity. In fig. 42b all concentric ellipses are similar (identical axial ratios) which implies increased separation along the parallel and decreased separation along the perpendicular radii. Comparisons with experiment reveals that the ring structure does indeed become somewhat more widely spaced along the parallel radii (figs. 5–10 and 33), but far from sufficient to be in accordance with fig. 42b. Accordingly only a small proportion of the elongation may be by the strictly affine mode of fig. 42b, and thus the different area elements cannot deform identically irrespective of their position in the spherulite.

Observations suggest both a higher degree of reorientation and deformation along the perpendicular radii compared with the parallel ones. We may consider the extreme case where deformations occur only in a perpendicular direction to the radius but not along it. This means that maximum deformation will occur along the perpendicular and none along the parallel radii. For the oblique ones the deformation will be proportional to the component of the radius perpendicular to the direction of draw. This mode of deformation will preserve the original ring separation all round the spherulite but cannot extend till near the centre where much enhanced elongation is required in order to preserve the continuity within the spherulite. This is embodied by *Wilchinsky*'s second alternative (fig. 42c) which, however, was arrived at by an argument which we consider fallacious. Comparison with observations shows that this model closely conforms to the deformation behaviour actually observed (e. g. figs. 6–12).

An important contrast between the deformation modes, fig. 42b and c, has already been pointed out by *Wilchinsky* (37), whose figure is here reproduced (fig. 43). We see that in the first case an originally straight radial line remains straight on deformation with altered length and orientation, but in the second case it becomes curved in addition, a point already raised when treating orientation effects along oblique radii.

As referred to earlier, at very high elongations all the regions along the parallel radii may become highly deformable as revealed by the pointed spherulite tips (figs. 10–12). In this case the model of fig. 42c is no longer adhered to in any portion of the spherulite.

The question arises whether the affine relation between an individual deformed

[1]) Attempts to do this directly on individual spherulites were made. It was found, however, that when the spherulite and collimator size are comparable the photographs obtained show additional complicating features. An account of these features will be given separately (36).

spherulite and the sample as a whole is preserved or not. While the deformation in fig. 42c is not affine in terms of the microstructure – i. e. the deformation of all the rings does not conform to that of the macroscopic dimensions of the specimen – the affine relationship may still hold for the outline of the spherulite as a whole. If it does it is unlikely to persist for the altered deformation mode at the high elongations (pointed tips) and vice versa. Unless the density is widely altered the affine condition must nevertheless be satisfied on some structural level larger than the spherulite if the spherulites themselves do not do so. Thus there should be groups or clusters of spherulites whose collective deformation conforms to that of the sample as a whole.

In the preceding considerations continuous orientation and deformation variations were implied. When going to the case of discontinuous yielding as approximated by the inhomogeneously deformed spherulites of figs. 2 to 3 it is apparent that yielding is favoured along the perpendicular radii. As regards the boundary of the yielded regions the following extreme cases can be considered:

i) The boundary is along a radial direction. In this case in order to maintain material continuity strain at the inner portions will have to become increasingly larger reaching infinity at the centre (fig. 19a). ii) The boundary is perpendicular to the direction of the tensile stress (fig. 19b). This will maintain uniform strain in the yielded portion. However, at the centre of the spherulite the initial orientation of the deformed region is approximately that of parallel radii whereas at the edges it is nearly perpendicular. Thus the centre is less favourably oriented for extension. Consequently a case intermediate between i) and ii) is expected. This again is at least consistent with observation. The inhomogeneous deformation of the spherulite clearly cannot be affine. Unless the affine requirement is satisfied on a larger scale (groups of spherulites) material continuity cannot be preserved. This latter alternative is found to be the case. Accordingly the longitudinal cracks and voids, seen in figs. 13–14, are direct consequences of the non-affine nature of the deformation. In more concrete terms, the narrowing at the central waist not being compensated by the widening in the adjacent material the gaps observed must necessarily result.

The behaviour of the exact centre is problematic. Geometrically, a spherical structure must have a singularity there. Physically this is not strictly true as the spherical symmetry is not preserved to the exact centre. Thus spherulite centres are sheaves fanning out gradually. The orientation of the sheaf axis with respect to the draw direction must be relevant to what happens at the spherulite centre on deformation. In our experimental material, we have no information on this point which would require special examination.

We now consider the effect of the radial periodicity on the dimensional changes. Should even only a broad correlation exist between orientation and deformation, this periodicity implies a varying amount of deformation along a given spherulite radius. Thus in the case of a perpendicular radius crystals $2_\perp$ undergo the maximum 90° c axis orientation change while crystals $1_\perp$ do not change at all (fig. 24). Clearly this cannot mean the absence of any deformation in the latter regions.

At this juncture the electron micrographs in figs. 33–36 are helpful. Fig. 35 is representative of a region comprising mainly perpendicular radii. The dark bands are the annulli where the lamellae are seen edge on, hence are close to positions $1_\perp$ in fig. 24. It can be seen that these regions elongate by the lamellae becoming progressively separated in an accordion fashion and presumably without any change in orientation. The transition from parallel to perpendicular radii can be seen from fig. 34. In the former region the lamellae as seen edgewise are closely together, while they become progressively separated when passing towards the perpendicular radii. Obviously as the lamellae are being separated some material in between must become stretched. The same feature emerges in detachment replicas of highly stretched samples (fig. 36). Here again we see dark lines which must represent thickening, hence presumably lamellae seen edge on, perpendicular to the draw direction. The frequency of these depends on the amount of stretching, or relaxation from the stretched state induced deliberately or accidentally in the course of specimen preparation. In either case the crystal orientation as revealed by the diffraction pattern is unaffected by the morphology (fig. 38). According to our picture this is due to the fact that the lamellae are already in the correct final alignment, only their separation is variable, which is also the situation in the dark regions of the perpendicular radii in fig. 35. All this

implies that deformation can occur unrelated to changes in crystal orientation, particularly when the *c* axis is already along or near the draw direction.

We conclude that orientation and deformation cannot be quantitatively related without detailed knowledge of the behaviour of the microstructure on the different levels laid out here. Any correlation constructed in the present state of knowledge of the morphology is deemed to be of limited validity if valid at all. This does not exclude the possibility that over a limited range of extensions the overall average orientation of the sample may be related to the extension analytically. However, in such averaging treatment, the real microstructural nature of both orientation and deformation is likely to be obscured. [It will only be mentioned that in some very specially prepared samples a meaningful correlation between crystal orientation (as assessed by discrete maxima along the azimuth in the diffraction patterns and not by forming averages, as in ref. 37) and elongation could be established (38, 39). These samples, however, were not directly spherulitic, and discussion of them will be deferred to a later publication].

It will be clear that a description of deformation in terms of crystal orientation alone cannot be fully adequate. But even in so far as a crystallographic description may suffice, this cannot consist of a mere bodily rotation of individual lamellae. In the final state the lamellae would be normal or, at any rate, at an angle less than 45° to the draw direction, i. e. with a short dimension along the direction of elongation, which cannot lead to an overall increase in length of the sample, unless the rotation of whole piles of lamellae longer than wide are invoked, which is certainly a possibility.

So far we have considered the deformation of a single separated spherulite. As an idealised case we may regard a system of isolated spheres surrounded by an isotropic matrix. Even under these simplified conditions the general stress-strain behaviour represents a complex problem. We are dealing with an aggregate where the spheres not only have a different stress/strain behaviour to the matrix but also different portions of the spheres behave differently. If, in addition, the spherulites are in contact, the problem becomes that of a polycrystalline aggregate. In this case, together with the usual difficulties encountered amongst simple materials, we have the added complication that, in general, regions having differing stress/strain behaviour will be in contact in adjacent spherulites, all contact combinations being realised. Accordingly there will be micro-inhomogeneity both of stress and strain. Taking the extreme cases, in some combinations of micro-regions the stress may remain unaltered and the strain is averaged (*Reuss* average) while in others there may be unaltered strain and averaged stress (*Voigt* average) with all cases in between. It is obvious therefore that the overall stress/strain behaviour of a spherulitic polymer is not likely to be accounted for by one simple model.

6.4. Non-crystallographic factors

It has been pointed out previously that the deformation behaviour cannot be fully accounted for by crystallographic factors alone. The most obvious indication of this was the insensitivity of the diffraction patterns to large changes in elongation in the highly oriented state. Another observation pointing the same way is the pronounced reversibility both in spherulite shape and crystal orientation. This requires large elastic deformations associated with a low modulus characteristic of rubber-like elasticity not found amongst crystals as such. So far the present paper has dealt strictly with observations and their direct assumption-free interpretation. When searching for the origin of the long range elasticity some speculative elements need necessarily to be introduced.

The material responsible for the non-crystallographic features may be an amorphous matrix in which the crystals are embedded, alternatively, it may be represented by tie molecules which connect the individual crystal lamellae or it may be a combination of both. Tie molecules may be of two kinds, those which are present in the undeformed material to begin with and those which are formed during deformation by chains being pulled out from the chain folded crystals. As will be discussed, this last process seems to play a significant part, but clearly some preexisting ties are required for it to operate.

The near reconstitution of the original spherulites from the highly deformed state (up to 5 X elongation) is very surprising. The fact that the sample not only retracts as a whole, but the appearance of the spherulite in itself is regenerated implies that the

crystals return to their original positions relative to each other. This means that neither the crystals themselves nor the links between them have been permanently disrupted, and that the crystals are merely displaced with respect to each other with strained material between them in which the restoring energy is accumulated. We were unable to pin down in any concrete structural or dimensional terms the limit where this spherulitic memory was finally lost. It occurred to some extent progressively. The inhomogeneously deformed material was certainly irreversible in this respect, and the inhomogeneous component certainly increased with elongation even in spherulites which we classed here as homogeneously deformed. Another criterion could be the randomisation around the *c* axis at high elongations. When this occurs the relation between the drawn structure and that of the original spherulite is lost, and reconstitution of the spherulite could hardly be expected. It is realised that the high reversibility observed here may well be the consequence of the special specimens used. Even if this were so we believe that the effect itself is a general one, being merely accentuated by the undoubtedly special nature of the sample. (Some retraction on removal of load is a familiar occurrence in the usual tensile testing. We find that this is characteristic of regions which have not necked, hence could correspond to the unyielded portions in the present experiments).

The highly drawn samples appear to consist partly at least of lamellae as seen edge-on (fig. 36). There is in fact mounting evidence of lamellae perpendicular to the draw direction being representative building units of even comparatively highly drawn fibres [*Hay* and *Keller* (40)]. The molecules are known to be perpendicular to the lamellae from the diffraction patterns (fig. 38) and in view of the fact that in the two-dimensional films such as in fig. 36 the lamellae (the thick lines) are at least partly separated entities the conclusion that they must consist to a large extent of folded molecules can hardly be avoided. This has the important implication that chain folding must exist even in highly drawn structures, the straight segments lying along the draw direction. The pulled out regions between the layers seen, e. g. in fig. 36b, could then correspond to the extended material originally between the lamellae plus material that pulled out from the crystals. In view of the fact that elongation increases at the expense of the lamellae – the thick lines in the photographs are getting fewer and shorter and the stretched material in between longer – we suggest that the crystals transform gradually into this interlamellar stretched material presumably by the pulling out of the folds. Accordingly the thin stretched regions would contain fewer or no folds.

Structures of the kind as in fig. 36 have been frequently observed in various polymers both as growth features or as resulting from deformation of single crystals. *Kobayashi* suggested that they are pulled out single crystals [private communication, *Geil* (8)]. Threads of beads were amongst the earliest observations in pulled out chain folded systems (41) and even at that time the bands were associated with the fold period. Later observations have revealed that such beaded threads are in fact similar to the strings of lamellae in question. Such structures arising from deformation of single crystals are now receiving much attention [*Geil* (42)].

The picture emerging is as follows. When the crystals are approximately in their final orientation (*c* axes along the draw direction) the folds start pulling out progressively. A few folds pulled out would allow large elongations while the bulk of the material still preserves its essentially chain folded character. Such a sample would consist of blocks of chain folded material with pulled out ties in between.

However, the two-stage replicas revealed that the surface of highly drawn material is smooth, the transverse lines of thickening in the detachment replicas being caused by involuntary heat annealing during the sample preparation (28). Similarly threads as obtained directly from single crystals by drawing can be smooth, but they become beaded or striated on head treatment [*Geil* (42)]. Further, low angle X-ray maxima which normally are indicative of chain folded lamellae are usually diffuse and weak in fibres as drawn. All this may be interpreted by the folds being pulled out. Alternatively it may be that the chain folded regions are broken up into small blocks which are displaced with respect to each other along the fibre direction in an irregular fashion leaving no striated appearance. On annealing, these blocks could come into register producing lamellae accounting for the morphological and low angle X-ray effects observed.

Once the molecules are extended one would not expect them to refold on heating. If, however, the crystalline extended chain material were highly strained (e. g. under compression by the stretched amorphous) or imperfectly

crystalline or both, it could melt at the annealing temperature and recrystallise in a folded form with the appropriate fold length. In the case of material beeing present in the folded form to begin with the annealing behaviour presents no special problem: the fold length would increase in a way familiar in chain folded systems in general.

It needs emphasising that all observations and deductions were made on two-dimensional spherulites. The three-dimensional spherulitic structure as present in the usual bulk material may well raise some additional problems and complete identification of the present findings with what might happen in the bulk proper requires caution. Unfortunately three-dimensional spherulites are not readily accessible to the present type of observation. *Langkammerer* and *Catlin* (12) prepared transverse sections of bulk filaments, the longitudinal sections of which had the appearance of our highly drawn samples. They state that these cross-sections show a circular symmetry which we would expect from a three-dimensional generalisation of our model.

6.5. Some additional points

The present observations have some further implications. The nonuniform response of the spherulites to deformation (both elastic and plastic) must have a profound effect on the interpretation of the mechanical properties as measured on the bulk as a whole. It is clear that such properties must be averages of those characteristic of the individual components. Similarly in time-dependent behaviour there must be different relaxation times associated with the deformation processes in the different portions of the spherulites. In this connection the remarkable recovery properties of the spherulites are significant. We see that different portions of the spherulites recover with different rates dependent on conditions of extension and relaxation. This must be associated with processes occurring between and within the lamellae and raises the possibility of accounting for some features of the mechanical relaxation spectrum in concrete structural terms. It is perhaps noteworthy that by special means fibres and films can be obtained possessing orientations which correspond to that along a spherulite radius [*Point* (38), *Keller* (43), *Takanayagi* (44)]. If this correspondence is also applied to the deformation behaviour it would follow that such films and fibres would deform as parallel spherulite radii in the present paper. Such special preparation could therefore be used as macroscopic models (as already done partly by *Point* (38) and work in progress by us) for determining the properties of such 'spherulite radii' quantitatively and thus give information on the basic constituent of which a bulk sample is composed. In view of the high resistance to deformation of the parallel radii the properties of such fibres may deserve special attention.

The inhomogeneously deformed samples in particular can be regarded as composite systems, consisting of highly deformed material with practically undeformed particles embedded within. From the point of view of mechanical behaviour these embedded regions may be considered as foreign inclusions. In this respect such samples resemble blends, where foreign particles are added on purpose, and may well need treating as such in their mechanical behaviour. A very obvious similarity is the crack formation usually accompanied by whitening of the material due to scatter of light, a familiar feature in blended amorphous polymers [e. g. polystyrene-rubber blends, *Haward* and *Mann* (45)]. Closer to our topic, longitudinal crack formation is a familiar observation in the drawing and stressing of crystalline, presumably spherulitic, materials [e. g. *Farrow* and *Ford* (46)]. We see that in our case this is due to the inhomogeneous deformation (micronecking) of spherulites, of which figs. 13–14 are two-dimensional representations. Accordingly the longitudinal voids observed in general could also be a consequence of the spherulitic microstructure, the continued study of which may promote their understanding and practical control. We also see that spherulites separating these voids appear to be ultimately responsible for fibrillation or tearing, the width of the fibrils correponding to that of the pulled out spherulites. Again, fibrillation is an intrinsic property of crystalline polymers and the significance of a connection with the spherulitic morphology needs no further emphasis.

Finally a brief comment on the highly drawn fibre. Firstly, we see that even highly drawn material may have some undrawn inclusions, the significance of which has just been raised. Secondly, figs. 16 and 17 imply that the intrinsic disorientation normally found in fibres need not consist of a statistical spread of orientation on a molecular scale

but can be due to microscopic regions which possess orientations slightly different from that of the fully aligned fibre, only the average of which is normally observed.

Conclusion

It emerges from the material presented that the deformation of a spherulitic polymer is a structurally complex process. It will be clear that any attempt to account for it in terms of a single mechanism based on some a priori consideration would be unprofitable. Neither does there seem to be much prospect to arrive at an adequate understanding of the microstructural processes from measurements of macroscopic properties alone as these can only provide averages from which the individual processes are unlikely to be extracted. There appears to be no substitute for a piece by piece unravelling of all factors by detailed microstructural studies. It is hoped that the present account has mapped out some principal avenues along which to proceed in this quest.

Acknowledgements

We wish to thank Mrs. *Gina Dyer* for her original contribution to the electron microscope sample preparation and Miss *Jean Robinson* for her invaluable technical assistance in preparing the illustrations.

Our thanks are due to Professor *F. C. Frank* for his interest and for numerous discussions.

Summary

A range of experimental material concerning the behaviour of spherulites on deformation of polyethylene is presented, systematised and evaluated. The techniques used comprise polarising microscopy, X-ray diffraction (macro and micro), electronmicroscopy and electron diffraction. Examples of different deformation modes of spherulites are shown dependent on the conditions of deformation of the specimen. The deformation of the spherulites can be homogeneous or inhomogeneous. In the former case different parts of the spherulite deform progressively in a constant ratio while in the latter some parts deform while others remain essentially unaffected. A large amount of reversibility is associated with the former mode. An extreme case of the latter mode is where deformation is confined to the spherulite boundary regions. In all cases non-identical behaviour is apparent for the same structural elements within the spherulite, but located in different positions with respect to the draw direction. There is a distinctly different behaviour between the radial elements lying at different angles to the draw direction and also between the elements within a radius (corresponding to the various phases of twist which characterises such a radius). It is shown that highly drawn material preserves some memory of the original spherulitic structure and further that void formation on drawing can arise as a direct consequence of the non-affine deformation of the spherulites.

The findings are analysed in some detail and most of the observations on the fine structure are accounted for in crystallographic terms. When considering the dimensional changes, however, non-crystalline rubbery components need also to be invoked which, to some extent, appear to be most significant. The possible relation of these observations to the chain folded lamellar crystallisation is indicated.

Zusammenfassung

Es wird ein Teil experimentellen Materials über das Verhalten von Sphärolithen bei Deformation von Polyäthylen dargestellt. Die angewendete Technik umfaßt Polarisationsmikroskopie, Röntgenstreuung (Weit- und Kleinwinkel-), Elektronenmikroskopie und Elektronenstreuung. An Beispielen verschiedener Deformationsart von Sphärolithen wird die Abhängigkeit von den Bedingungen der Deformation der Proben gezeigt. Die Deformation der Sphärolithe kann homogen und inhomogen erfolgen. Im ersteren Fall verformen sich Teile des Sphärolithen progressiv im konstanten Verhältnis, während im letzteren Fall einige Teile sich verformen und andere im wesentlichen unbeeinflußt bleiben. Ein wesentlicher Anteil der Reversibilität ist mit der 1. Art der Verformung verknüpft. Ein Extremfall der letzten Verformungsart ist der, in dem die Deformation auf die Sphärolithgrenzen beschränkt ist. In allen Fällen scheint nichtidentisches Verhalten für gleiche Strukturelemente innerhalb der Sphärolithe vorzuliegen, insofern diese in verschiedener Lage hinsichtlich der Zugrichtung stehen. Es ist ein deutlich unterschiedliches Verhalten innerhalb von Radialelementen von verschiedenem Winkel zur Zugrichtung und auch innerhalb eines der auf einem Radius liegenden Elemente festzustellen. Letzteres entspricht den verschiedenen Phasen der Verdrillung, die längs einem solchen Radius auftreten.

Es wird gezeigt, daß hochverstrecktes Material ein gewisses Gedächtnis für die ursprüngliche Struktur behält und ferner, daß Hohlstellenbildung beim Verstrecken als unmittelbare Folge nicht-affine Deformation der Sphärolithe bedingen kann.

Diese Ergebnisse werden im Detail analysiert und der größte Teil der Beobachtung der Feinstrukturen läßt sich in kristallographischen Größen ausdrücken.

Wenn man jedoch die Dimensionsänderung betrachtet, müßten nichtkristalline gummiähnliche Anteile herangezogen werden, welche bis zu einem gewissen Grad sehr wichtig erscheinen. Die mögliche Beziehung dieser Beobachtungen zu der Faltungskristallisation wird aufgezeigt.

References

1) *Keith, H. D.* and *F. J. Padden*, J. Polymer Sci. **41**, 525 (1959).

2) *Sasaguri, K., S. Hoshino* and *R. S. Stein*, J. Appl. Phys. **35**, 47 (1964).

3) *Erhardt, P., K. Sasaguri* and *R. S. Stein*, J. Polymer Sci. C **5**, 179 (1964).

4) *Stein, R. S., S. Onogi, K. Sasaguri*, and *D. A. Keedy*, J. Appl. Phys. **34**, 80 (1963).

5) *Yu, Y. F.* and *R. Ullman*, J. Polymer Sci. **60**, 55 (1962).

6) *Ingram, P.* and *A. Peterlin*, J. Polymer Sci. **B 2**, 739 (1964).

7) *Cooney, J. L.*, J. Appl. Polymer Sci. **8**, 1889 (1964).

8) *Geil, P. H.*, Polymer Single Crystals, Interscience (New York, London 1963).

9) *Barish, L.*, J. Appl. Polymer Sci. **6**, 617 (1962).

10) *Jenckel, E.* and *E. Klein*, Kolloid-Z. **118**, 86 (1950).

11) *Bryant, W. M. D.*, J. Polymer Sci. **2**, 247 (1947).

12) *Langkammerer, C. M.* and *W. F. Catlin*, J. Polymer Sci. **3**, 305 (1948).
13) *Hammer, C. F., T. A. Koch* and *J. F. Whitney*, J. Appl. Polymer Sci. **1**, 164 (1959).
14) *Keller, A.*, J. Polymer Sci. **17**, 291 (1955).
15) *Keller, A.* and *J. R. S. Waring*, J. Polymer Sci. **17**, 447 (1955).
16) *Point, J. J.*, Bull. Acad. roy. Belg. **41**, 947 (1955).
17) *Keller, A.*, J. Polymer Sci. **39**, 151 (1959).
18) *Keith, H. D.* and *F. J. Padden*, J. Polymer Sci. **39**, 101 (1959).
19) *Price, F. P.*, J. Polymer Sci. **37**, 71 (1959).
20) *Fischer, E. W.*, Kolloid-Z. **159**, 108 (1958).
21) *Brown, A.*, J. Appl. Phys. **20**, 552 (1949).
22) *Keller, A.*, J. Polymer Sci. **15**, 31 (1955).
23) *Horsley, R. A.* and *H. A. Nancarrow*, Brit. J. Appl. Phys. **2**, 345 (1951).
24) *Keller, A.*, J. Polymer Sci. **17**, 351 (1955).
25) *Bassett, D. C.*, Phil. Mag. **6**, 1053 (1961).
26) *Keller, A.* and *D. C. Bassett*, J. Roy. Microscop. Soc. **79**, 243 (1960).
27) *Palmer, R. P.* and *A. J. Cobbold*, Makromol. Chem. **74**, 174 (1964).
28) *Bassett, G. A.* and *A. Keller*, Phil. Mag. **9**, 817 (1964).
29) *Keller, A.* and *S. Sawada*, Makromol. Chem. **74**, 190 (1964).
30) *Hendus, H.*, Kolloid-Z. **165**, 32 (1958).
31) *Bunn, C. W.*, Trans. Faraday Soc. **35**, 482 (1939).
32) *Frank, F. C., A. Keller* and *A. O'Connor*, Phil. Mag. **4**, 200 (1959).
33) *Bassett, D. C., F. C. Frank* and *A. Keller*, Phil. Mag. **8**, 1739 (1963).
34) *Turner-Jones, A.*, J. Polymer Sci. **62**, S 56 (1962).
35) *Geil, P. H.*, J. Polymer Sci. **A 2**, 3813 (1964).
36) *Hay, I. L.* (to be published).
37) *Wilchinsky, Z. W.*, Polymer **5**, 271 (1964).
38) *Point, J. J.*, Memoires et Publications de la Société des Sciences des Arts et Lettres du Hainaut **71**, 65 (1958).
39) *Hay, I. L., T. Kawai*, and *A. Keller*, International Symposium on Macromolecules Chemistry, Prague 1965. Preprint No. P 325.
40) *Hay, I. L.* and *A. Keller*, Nature **204**, 862 (1964).
41) *Keller, A.*, Phil. Mag. **2**, 1171 (1957).
42) *Geil, P. H.*, J. Polymer Sci. **A 2**, 3835 and 3857 (1964).
43) *Keller, A.*, J. Polymer Sci. **21**, 363 (1955).
44) *Takanayagi, M.*, Memoirs of the Faculty of Engineering, Kyushu University **23**, 41 (1963).
45) *Haward, R. N.* and *J. Mann*, Proc. Roy. Soc. **A 282**, 120 (1964).
46) *Farrow, B.* and *J. E. Ford*, Nature **201**, 183 (1964).

Authors' address:
J. L. Hay and Dr. *A. Keller*
H. H. Wills Physics Laboratory, University, Bristol (England)

Aus dem Institut für Kunststoffe der Deutschen Akademie der Wissenschaften zu Berlin

Dielektrische Untersuchungen an Polyvinylacetat während der isothermen Volumenkontraktion

Von Siegfried Kästner und Manfred Dittmer

Mit 5 Abbildungen

(Eingegangen am 14. Juni 1965)

Einleitung

Zur Deutung des dielektrischen Verhaltens der amorphen Polymeren im Hauptrelaxationsgebiet kann oberhalb der Glastemperatur sowohl die Theorie der gekoppelten Potentialmuldenübergangsprozesse (1–4) als auch die Theorie der vom freien Volumen gesteuerten Diffusionsprozesse (5–8) herangezogen werden. Beide Theorien enthalten bezüglich der mittleren Relaxationszeit τ_m zwei wesentliche Konstanten, wodurch mit den im begrenzten Temperaturbereich gewonnenen Meßergebnissen stets eine befriedigende Übereinstimmung erzielt werden kann. Eine Entscheidung zwischen beiden Theorien ist nur möglich, wenn man das dielektrische Verhalten unterhalb bzw. in der Umgebung der Glastemperatur untersucht. Das freie Volumen befindet sich nämlich nur oberhalb der Glastemperatur im Gleichgewicht, während es sich unterhalb und in der Umgebung der Glastemperatur nur in einem Relaxationsvorgang dem Gleichgewicht nähert, wobei die Relaxationszeit mit abnehmender Temperatur sehr stark anwächst (9). Dieser Relaxationsvorgang des freien Volumens muß sich aber auch im dielektrischen Verhalten äußern, falls es sich hierbei um einen vom freien Volumen gesteuerten Diffusionsprozeß handelt.

Die entsprechende Theorie ergibt für die Frequenz ν_m des Maximums des Imaginärteils ε'' der komplexen Dielektrizitätskonstante $\varepsilon^* = \varepsilon' - i\,\varepsilon''$ den Zusammenhang

$$\nu_m = \nu_{m\infty}\, e^{-B/f}, \qquad [1]$$

der neben den Konstanten $\nu_{m\infty}$ und B das relative freie Volumen f enthält, für das allgemein die lineare Beziehung

$$f = f_0 + \alpha_f (T - T_0) + \Delta f \qquad [2]$$

verwendet wird. Dabei kennzeichnet f_0 den Gleichgewichtswert des freien Volumens bei